Mimicking the Structure of the V3 Epitope Bound to HIV-1 Neutralizing Antibodies[†]

Amit Mor,[‡,#] Eugenia Segal,[‡,#] Brenda Mester,[#] Boris Arshava,[§] Osnat Rosen,[#] Fa-Xiang Ding,[§] Joseph Russo,[§] Amnon Dafni,[#] Fabian Schvartzman,[#] Tali Scherf,[||] Fred Naider,[§] and Jacob Anglister*[,#]

Department of Structural Biology and Chemical Research Support Weizmann Institute of Science, Rehovot 76100, Israel, and Department of Chemistry, College of Staten Island of the City University of New York, Staten Island, New York 10314

Received December 18, 2008; Revised Manuscript Received March 12, 2009

ABSTRACT: The third variable region (V3) of the HIV-1 envelope glycoprotein gp120 is a target for virus neutralizing antibodies. The V3 sequence determines whether the virus will manifest R5 or X4 phenotypes and use the CCR5 or CXCR4 chemokine coreceptor, respectively. Previous NMR studies revealed that both R5- and X4-V3 peptides bound to antibodies 0.5β and 447−52D form β-hairpin conformations with the GPGR segment at the turn. In contrast, in their free form, linear V3 peptides and a cyclic peptide consisting of the entire 35-residue V3 loop were highly unstructured in aqueous solution. Herein we evaluated a series of synthetic disulfide constrained V3-peptides in which the position of the disulfide bonds, and therefore the ring size, was systematically varied. NMR structures determined for singly and doubly disulfide constrained V3-peptides in aqueous solution were compared with those found for unconstrained $V3_{JRFL}$ and $V3_{IIIB}$ peptides bound to 447−52D and to 0.5β, respectively. Our study indicated that cyclic V3 peptides manifested significantly reduced conformational space compared to their linear homologues and that in all cases cyclic peptides exhibited cross-strand interactions suggestive of β-hairpin-like structures. Nevertheless, the singly constrained V3-peptides retained significant flexibility and did not form an idealized β-hairpin. Incorporation of a second disulfide bond results in significant overall rigidity, and in one case, a structure close to that of $V3_{MN}$ peptide bound to 447−52D Fab was assumed and in another case a structure close to that formed by the linear $V3_{IIIB}$ peptide bound to antibody 0.5β was assumed.

The third variable region (V3) of the HIV-1 envelope glycoprotein gp120 is involved in gp120 binding to the chemokine receptors CCR5 and CXCR4, which serve as coreceptors in HIV-1 infection. The sequence of V3 determines whether the virus binds to CCR5 and infects predominantly macrophages ("R5 virus") or to CXCR4 and infects mostly T-cells ("X4 virus"). The V3 loop has been previously termed as the "principal neutralizing determinant" of HIV-1, since many HIV-1 neutralizing antibodies from infected individuals target this region of gp120 (*1*). Such antibodies prevent the binding of gp120 to the chemokine receptors, thus blocking events leading to viral fusion (*2, 3*). V3 peptides have been investigated as a potential anti-HIV-1 vaccine, and a few studies using HIV-1 and SHIV V3 peptides have demonstrated the induction of antibodies that neutralize homologous HIV-1 primary isolates (*4*−*8*). Recently, a 22-residue V3 segment (in the form of a C4−V3 peptide, where C4 stands for the fourth constant region of gp120), that resembles the consensus sequence of clade-B R5 viruses, was found to induce antibodies that neutralized 31% of the subtype-B HIV-1 isolates evaluated (*9*).[1]

Linear V3 peptides are mostly flexible in solution, and except for a β-turn formed by the GPGR segment, no well-defined secondary structure has been observed (*10, 11*). As a result of this flexibility, we assume that linear V3 peptides used as immunogens will induce a wide spectrum of antibodies, most of which will not recognize the native conformation of the corresponding region in gp120. It is plausible that peptides designed to mimic the native conformation of the antigenic determinant presented by gp120

[†] This study was supported by NIH Grant GM53329 (J.A.) and GM22086 (F.N.), and by the Horowitz Foundation, Gurwin Foundation and the Kimmelman Center. J.A. is the Dr. Joseph and Ruth Owades Professor of Chemistry and F.N. is the Leonard and Esther Kurtz Term Professor at the College of Staten Island at the City University of New York.

* To whom correspondence should be addressed. E-mail: Jacob.Anglister@weizmann.ac.il. Phone: 972-8-9343394. Fax: 972-8-9344136.

[‡] These authors contributed equally to the study.

[#] Department of Structural Biology, Weizmann Institute of Science.

[||] Chemical Research Support, Weizmann Institute of Science.

[§] College of Staten Island of the City University of New York.

[1] Abbreviations: DQF-COSY, Double Quantum Filtered COrrelated SpectroscopY; EDT, 1,2 ethanedithiol; ELISA, enzyme-linked immunosorbent assay; ESI-MS, electrospray ionization mass spectrometry; HOHAHA, HOmonuclear HArtman-HAnn; HRP, Horseradish peroxidase; MALDI-TOF, matrix assisted laser desorption /ionization- time of flight mass spectrometry; NOEs, NOE interactions; NMP, *N*-methyl pyrrolidone; $NN_{i,i+1}$ ($\alpha N_{i,i+1}$), HN-HN (Hα-HN), NOE interactions between adjacent residues; NOESY, nuclear Overhauser effect spectroscopy; rmsd, root mean square deviation; sCD4, a soluble CD4 fragment consisting of two extra-cellular immunoglobulin domains of CD4; TFA, trifluoroacetic acid; TIS, triisopropylsilane; $V3_{XXX}$, V3 of the xxx strain; $V3_{X\#\#\#C-Y\#\#\#C}$, constrained V3 peptide in which residues X and Y (at positions ###) were replaced by cysteines and oxidized to a disulfide bond connecting these positions; WATERGATE, WATER suppression by GrAdient Tailored Excitation.

10.1021/bi802308n CCC: $40.75
Published on Web 03/13/2009

will be more potent in eliciting antibodies that are cross-reactive with HIV-1. Although gp120 and mixtures of gp120 from various strains could be potential vaccine candidates, peptide-based vaccines have numerous advantages including ease of preparation, stability, and cost in comparison to those based on the intact protein.

To gain insights into the conformation of the V3 region presented to the immune system by HIV-1, we previously studied the structures of V3 peptides bound to the HIV-1 neutralizing antibodies 0.5β and 447−52D (*12*). The murine monoclonal antibody 0.5β, generated against gp120 of the X4 virus HIV-1_{IIIB}, is a very potent strain-specific HIV-1 neutralizing antibody (*13*). The second antibody 447−52D is a human monoclonal antibody derived from an HIV-1 infected donor (*14*), and therefore the exact strain that elicited its production is unknown. This antibody is one of the most potent HIV-1 neutralizing antibodies directed against V3. It neutralizes 45% of clade-B isolates and is capable of neutralizing both X4 and R5 viruses as well as many primary isolates (*15, 16*).

The structure of a $V3_{IIIB}$ peptide (V3 region of the IIIB strain) in complex with the 0.5β antibody Fv and the structure of three different V3 peptides corresponding to IIIB, MN, and JR-FL sequences in complex with 447−52D Fv were determined by NMR (*17*−*21*). All bound V3 structures showed a β-hairpin conformation and an rmsd between the hairpin regions of any two V3 structures in the different complexes ranging between 1.2 and 2.5 Å. An extended conformation of the V3 N-terminal strand and a β-turn formed by the GPGR segment was observed also in crystallographic studies of V3 complexes with the Fab fragments of other HIV-1 neutralizing antibodies (*22*−*28*). In all NMR and crystallographic studies of V3 peptides in complex with Fv or Fab fragments of different HIV-1 neutralizing antibodies, the N-terminal segment of the V3 and the GPGR segment formed extensive interactions, while the C-terminal segment exhibited considerably fewer interactions with the antibodies (*17, 19*−*23, 25, 28*). Two different N-terminal strand conformations have been observed: one that is recognized by the 0.5β antibody (*19*) and the other recognized by the 447−52D antibody (*17, 20, 21*). These two conformations differ by a one register shift in the N-terminal strand residues that form hydrogen bonds within the β-hairpin and a 180° shift in the orientation of the side chains (*17*). We postulated that the $V3_{IIIB}$ conformation bound to the 0.5β Fv represents the X4 conformation of the V3, while conformations of V3 peptides bound to 447−52D represent the R5 conformation (*17*). The conformation of $V3_{JR\text{-}FL}$ and $V3_{IIIB}$ bound to 447−52D differ from that of $V3_{MN}$ recognized by the same antibody in the pairing of the residues in the β-hairpin, resulting in a further differentiation to $R5_A$ ($V3_{MN}$) and $R5_B$ ($V3_{JR\text{-}FL}$, $V3_{IIIB}$) substructures (*20, 21*).

Two crystal structures of gp120, containing the V3 region, in complex with a soluble CD4 extracellular fragment, sCD4, and an HIV-1 neutralizing antibody were published recently (*29, 30*). The rmsd between the Cα atoms of the V3 structure in the complex of gp120 with the HIV-1 neutralizing antibody X5 (*29*) and the Cα atoms of the NMR structure of $V3_{JR\text{-}FL}$ bound to 447−52D Fv (*21*) is 4.2 Å for residues 304−322. However, in the later crystal structure of gp120 in complex with the antibody 412d which contains tyrosine sulfated residues and interacts with the base of the V3 (*30*), the V3 structure shows remarkable agreement with the NMR structure with an rmsd of 1.6 Å for the Cα atoms of residues 304−322.

The NMR structure of the antibody bound conformation of the V3 could serve as a template for the development of constrained V3-peptide immunogens as potential candidates for an anti-HIV-1 vaccine. A number of approaches can be used to constrain peptides to the β-hairpin structures revealed in our previous NMR structure of antibody/V3 complexes. These include insertion of β-turn stabilizing motifs such as D-Pro-Gly and Asn-Gly (36,37) and cross-strand covalent linkages via amide or disulfide bonds (*31*). The design of constrained V3-peptides, mimicking a β-hairpin conformation, should consider the register of the hydrogen-bond-forming positions, especially in the N-terminal strand, and the pairing of the residues in the β-hairpin conformation. The use of a disulfide bond between the two β-hairpin strands can dictate both the specific pairing of opposing resides and the alignment of the hydrogen bond-network. Statistical analysis of protein structures revealed that cysteines occupy only those positions within the β-hairpin that do not form hydrogen bonds (*32*). Varadarajan and co-workers (*33*) relied on this observation and used a disulfide bond to constrain the 447−52D V3-epitope inserted at the tip of a thioredoxin β-hairpin. The constrained V3-thioredoxin molecule bound 447−52D with affinity comparable to that of gp120. However, structural studies of this V3 construct have not been reported. Moreover, this V3-construct failed to elicit HIV-1 neutralizing antibodies (*33*).

In earlier pioneering studies Conley and co-workers immunized rabbits and monkeys with cyclic V3 peptides corresponding to either HIV-1_{IIIB} or HIV-1_{MN} laboratory adapted X4 strains (*34*). The longest $V3_{IIIB}$ peptide 306SIRIQRGPGRAFVTIG^{321}, consisting of 16 $V3_{IIIB}$ residues, elicited sera that neutralized HIV-1_{IIIB} at titers ranging from 1:320 to 1:2560 but did not neutralize HIV-1_{MN}. The longest $V3_{MN}$ peptide 301YNKRKRIHIGPGRAFYTTNKIIG^{325}, consisting of 23 V3 residues, elicited antisera that neutralized HIV-1_{MN} in titers of 1:160−1:640 but neutralized HIV-1_{IIIB} only at a 10-fold higher concentration. The $V3_{MN}$ antisera neutralized also AL-1 and SF-2 but not four other strains. Shorter peptides elicited considerably poorer neutralizing antibody responses. Later attempts to use constrained V3 peptides for immunization (*33, 35*) yielded considerably poorer neutralization results in comparison with the experiments of Conley and co-workers. Thus, although conflicting results have been reported it is clear that properly designed constrained V3 antigens can result in HIV-1 neutralizing antisera.

Another approach to constrain the conformation of the V3 is to insert V3 segments into permissible loops of other proteins. Several studies investigated the immunogenicity and the HIV-1 neutralizing antibody response elicited by immunogens in which the entire V3 loop or segments of it were inserted into permissible locations in proteins such as *Pseudomonas* exotoxin (*36*), hepatitis B surface antigen (*37*), cholera toxin (*38*) and the tandem repeat protein of human mucine 1 (*39*). In other studies short V3 segments (7−12 residue long segments encompassing the GPGR sequence) or the entire V3 were inserted into viruses (*40, 41*), filamentous bacteriophage (*42*), or bacteria (*43*). In some of these studies an HIV-1 neutralizing antibody response was demonstrated. At the time these studies were carried out the

β-hairpin conformation of the V3 was not known; therefore, they did not attempt to mimic it. Nevertheless, in the context of the chimeric protein it is likely that some conformation was induced, especially for the short V3 segments. A more recent study used the entire V3 loop with a disulfide bond at its base fused to a carrier protein as an immunogen to elicit HIV-1 neutralizing antibodies (*44*). The entire consensus V3 sequences of clades A, B, and C R5 viruses were used in the construction of the immunogens. In this study the structure of the V3 in the immunogen was not determined; however, earlier NMR studies of peptides representing the entire length of the V3 loop and constrained through the native disulfide bond at the base of the V3 indicated that a β-hairpin conformation was not present (*11, 45, 46*). Although more flexible than the V3 segment used by Varadarajan and co-workers, the immunogen containing the entire V3 constrained only by the disulfide bond at its base was able to elicit antibodies that neutralized neutralization sensitive clade B viruses (*44*).

The previous studies described above have demonstrated that a potent HIV-1 neutralizing antibody response can be elicited using V3 immunogens. In contrast, it has proven to be very difficult to elicit HIV-1 neutralizing antibodies against gp120 and gp41 conserved epitopes similar to those determinants recognized by 2F5, 4E10, b12, and 2G12 (*47*−*50*). To make the V3 loop a viable vaccine candidate additional obstacles such as the occlusion of V3 in many primary isolates and its sequence variability have to be overcome. The synergism between soluble CD4 and CD4-mimic compounds may be used to increase the potency of V3-directed antibodies against HIV-1 strains in which the V3 is occluded (*51*−*53*) and the use of properly designed cocktails of V3-peptide immunogens may overcome the sequence variability of the V3.

As part of our program to develop a rational strategy to design peptide-based anti-HIV-1 vaccines, we are evaluating the structure of constrained V3 immunogens. The constrained V3-peptides have been designed on the basis of knowledge gained from our NMR studies. In side by side studies we are comparing the immunogenicity of these constrained and linear peptides, their binding to the 447−52D antibody and their propensity to assume specific structures in solution by NMR approaches. Herein we report results from NMR investigations on V3 peptides constrained by one or two disulfide bonds or D-Pro. Our results show that cyclic peptides with single disulfide bonds have a significantly higher propensity to form β-hairpin-like structures than the linear homologue. The closer the disulfide bond is to the GPGR turn, the more stable is the β-hairpin. Incorporation of a second disulfide bond results in significant overall rigidity, and in one case, a structure close to that of $V3_{MN}$ peptide bound to 447−52D Fab was assumed (R5A conformation) and in another case a structure close to that formed by the linear $V3_{IIIB}$ peptide bound to antibody 0.5β was assumed (X4 conformation).

EXPERIMENTAL PROCEDURES

Peptide Chain Assembly and Cleavage. Peptides were synthesized using solid-phase peptide synthesis with fluorenylmethoxycarbonyl (Fmoc) protection at the α-amine. Chain assembly was carried out either on a 443A peptide synthesizer (Applied Biosystems) using 0.1 mmol fast (Fmoc) chemistry or using an ABIMED AMS-422 automated solid-phase multiple peptide synthesizer (Langenfeld, Germany) on a 25 μmol scale. A Wang resin loaded with the appropriate *N*-Fmoc protected C-terminal amino acid was used to initiate the syntheses. Side chain protections were Lys(*t*-Boc), Asn(Trt), Cys(Trt) or Cys(Acm), Gln(Trt) His-(Trt), Asp(O-*t*-But), Glu(O-*t*-But), Ser(*t*-But), Tyr(*t*-But), Thr(*t*-But), and Arg(Pbf). Double coupling of each residue was carried out using either HBTU/HOBT in NMP (443A synthesizer) or benzotriazole-1-yl-oxy-tris-pyrolidino-phosphonium hexafluorophosphate in dimethylformamide (AMS-422 synthesizer) as the coupling agent. Four (AMS-422) to 10 (443A) equivalents of each Fmoc amino acid were used for coupling. In the 443A protocol capping of unreacted amino groups with acetic anhydride was used after every amino acid coupling step. All protected amino acids and coupling reagents were purchased from Advanced ChemTech or Novabiochem (Laufelfingen, Switzerland). Synthesis grade solvents were used in all procedures. Cleavage of the peptides from the Wang resins was performed using trifluoroacetic acid water cocktails [TFA/H_2O/EDT/TIS (94/2.5/2.5/1, v:v)] for 2 h at room temperature. The cleaved peptides were precipitated and washed with ice-cold ethyl ether, recovered by centrifugation, dissolved in acetonitrile/water (1:3 v:v), and lyophilized.

Isolation of Linear Peptides. All linear peptides were purified by preparative HPLC using Waters C-18 DeltaPak column 19 × 300 mm, 20 to 60% acetonitrile/water (0.1% TFA) gradient over 90 min at 5 mL/min flow rate. Collected fractions were analyzed by analytical HPLC and pooled to obtain better than 90% pure peptide for subsequent cyclization.

Cyclization of Peptides. The disulfide bond in peptides containing two cysteine residues were formed using either ferricyanide assisted cyclization or glutathione assisted oxidation reactions. All cyclizations were carried out at high dilution. In the first case to a solution of >90% pure linear peptide in 0.1 M ammonium acetate buffer pH 7.6 a stock solution of potassium ferricyanide was added (to the final concentration 0.17 mg/mL of peptide and 0.18 mg/mL ferricyanide) and the resulting solution was stirred at room temperature overnight. For the glutathione assisted oxidation the >90% pure linear peptide was dissolved at ∼1 mg/mL concentration in water containing 0.1% trifluoroacetic acid and the resulting solution was added dropwise to an 0.1 M ammonium acetate buffer pH 7.8 containing 0.5 mg/mL of L-glutathione and 0.1 mg/mL of oxidized L-glutathione, respectively to the final peptide concentration ∼0.05 mg/mL. The resulting solution was stirred at room temperature overnight. The progress of the reaction was judged using analytical HPLC and MS analysis. In many cases the cyclic and linear peptides were not distinguishable by HPLC. At the appropriate time, the reaction solution was acidified by trifluoroacetic acid to pH 4 and filtered, and the product was isolated by preparative HPLC. The entire cyclization reaction mixture, without further treatment, was injected onto the HPLC column equilibrated with 0.1% aqueous TFA and the column was washed with water until ferricyanide or glutathione eluted. A 0% to 50% acetonitrile/water (+0.1% TFA) gradient was applied to obtain products that were greater than 95% homogeneous as judged by analytical HPLC on Zorbax Eclipse XDB-C8 reversed phase columns

Table 1: Sequences of Peptides Used in the Study[a]

name of peptide	sequence	constrained to
V3 linear peptide	TRKSIHIGPGRAFYTTGEI	
Peptides constrained with one disulfide bond or D-Pro		
$V3_{entire}$	**C**TRPNNNTRKSIHIGPGR-AFYTTGEIIGDQAH**C**	
$V3_{T303C-I323C}$	**C**RKSIHIGPGRAFYTTGE**C**	R5B
$V3_{T303C-E322C}$	**C**RKSIHIGPGRAFYTTG**C**	R5A
$V3_{R304C-G321C}$	T**C**KSIHIGPGRAFYTT**C**E	X4
$V3_{K305C-T320C}$	RR**C**SIHIGPGRAFYT**C**GER	R5A
$V3_{I307C-T319C}$	TRKS**C**HIGPGRAFY**C**TGEI	R5B
$V3_{D-Pro}$	TRKSIHIG(D-P)GRAFYTTGEI	
Peptides constrained with two disulfide bonds		
$V3_{T303C-E322C;I309C-A316C}$	**C**RKSIH**C**GPGR**C**FYTTG**C**	R5A
$V3_{R304C-G321C;H308C-F317C}$	G**C**KS**I**C**I**GPGRA**C**YTTCG	R5A

[a] Replacement to cysteine is indicated by bold. Underlined residues indicate non-native residues added to increase solubility.

using an acetonitrile/water gradient in 0.1% TFA. The yields of the cyclization reaction, including purification varied from 25−50%. The final products were characterized by ESI-MS or MALDI-TOF and found to have a mass that differed by 2 Da from that of the linear homologue.

For peptides containing two disulfide bonds a combination of trityl (Trt) and acetamidomethyl (Acm) protection groups was chosen to selectively protect the cysteines so that the disulfide bond formation was predetermined. The two cysteines at the N and C termini were protected with Trt and the two inner cysteines with Acm. The trityl group is labile to TFA and was consequently removed during the normal course of the cleavage reaction, while the Acm is stable to the conditions required for the cleavage and removal of all other protecting groups. The first disulfide bond was formed by air oxidation after selective removal of Trt and purified as described above. The second disulfide bond was generated in a single step by treatment of the Acm protected peptide with iodine, using aqueous acetic acid as solvent to limit iodination of Tyr and Cys (*54*). The reaction was monitored by analytical HPLC and when completed, quenched with ascorbic acid (1 N). The reaction mixture was lyophilized and the crude mixture was purified using preparative reverse-phase HPLC. The final product with two disulfide bonds was >95% pure and had a molecular weight that was 4 Da lower than that of the completely linear precursor. The overall yield of the double disulfide peptide was 10−15% based on the linear precursor.

A list of all peptides investigated in the present study is given in Table 1. The nomenclature used in this paper reflects the positions of the cysteine substitutions used to form the disulfide bond and is indicated in the second column of Table 1. The numbering system used for the V3 peptides follows that suggested by Ratner et al. (*55*).

NMR Sample Preparation. Constrained V3 peptides (Table 1) were dissolved in a solution of 10 mM NaH_2PO_4 buffer containing 95% H_2O/5% D_2O, pH 6.0, and 0.05% NaN_3 at concentration ranging between 0.65−2 mM. Sample volumes were adjusted to 350 μL and the samples were placed into a Shigemi NMR test tube.

NMR Measurements. All NMR spectra were acquired on a Bruker DRX 800 MHz spectrometer using an inverse, triple resonance either room-temperature or Cryo probes, equipped with gradients. All measurements were performed at 273.5−277 K. The pulse sequence of the 2D HOHAHA (*56*) measurements used a WALTZ (*57*) or DIPSI-2 (*58*) sequence for isotropic mixing. The DQF-COSY spectra were acquired according to standard procedures (*59*). Water suppression schemes used in our NMR experiments included either WATERGATE, 3−9−19 or excitation sculpting sequences (*60*−*62*). Mixing times used for the NOESY experiments were 400 ms for $V3_{T303C-E322C}$. To avoid any possibility of spin diffusion shorter mixing times were used for the other peptides, 200 ms for $V3_{T303C-I323C}$, 250 ms for $V3_{R304C-G321C}$, 45−200 ms for $V3_{K305C-T320C}$ and 200 ms for $V3_{I307C-T319C}$. The spectra were processed using the NMRPipe (*63*) and XWIN-NMR (Bruker BioSpin DE) software. All data were analyzed using the NMRView (*64*) and the AURELIA software packages (Bruker BioSpin DE) (*65*).

Table 2: Experimental NMR Data and Structural Statistics of $V3_{R304C-G321C}$ and $V3_{I307C-T319C}$

	$V3_{R304C-G321C}$	$V3_{I307C-T319C}$
NMR distance constraints		
total	191	221
medium and long-range	52	67
torsion angle	0	0
hydrogen bond	5	1
mean rmsd values, Å		
all backbone atoms	1.72 ± 0.50	0.51 ± 0.17
all heavy atoms	2.16 ± 0.48	1.00 ± 0.30
distance constraint violation[a]		
no. > 0.1 Å	0	0
maximum (Å)	0	0
torsion angle violation[a]		
no. > 5°	0	0
maximum (deg.)	0	0

[a] The values given are the average and the standard deviation over the 20 energy-minimized conformers with the lowest residual CYANA target function values that represent the NMR solution structure.

Measurements of Temperature Coefficients. To examine the temperature dependence of the deviations of δH^N and the δH^α chemical-shift from random coil values, we measured HOHAHA spectra at 277, 285, 293, 300, and 308 K and acquired them as described above. $\Delta(\delta H^N)/\Delta T$ [ppb/K] ("temperature coefficient") values were calculated from the slope of the line that was fitted to the values of δH^N as a function of the measurement temperature. An H^N atom with temperature coefficient more positive than −4.5 [ppb/K] was assumed to be a hydrogen-bond donor. The hydrogen bonds identified in these measurements were used in the calculation of the NMR-based structures of the peptides.

Structure Calculation. $^3J_{HNH\alpha}$ coupling constants were determined whenever possible from the DQF-COSY spectrum, by the measurement of the separation between Lorentzian-fitted antiphase doublets using AURELIA (Bruker BioSpin DE). Automated NOE cross-peak assignments and structure calculations of the $V3_{R304C-G321C}$, $V3_{I307C-T319C}$, and $V3_{R304C-G321C;H308C-F317C}$ peptides were performed using the *'neoassign'* module of the CYANA 2.0 software (*66*). We used this program because of its ability and efficiency to handle in an unbiased manner quite large numbers of overlapping NOE cross-peaks and multiple assignment possibilities. Input files for the structure determination consisted of [^{1}H−^{1}H] chemical-shift lists, manually picked NOE cross-peaks and their intensities (from the H_2O NOESY spectra), and dihedral angle constraints derived from the $^3J_{HNH\alpha}$-couplings (*67*). Default parameters were used in all calculations. The final cycle in each run was set to yield an ensemble consisting of 20 energy-minimized structures. The final assignment of the NOE cross-peaks was checked

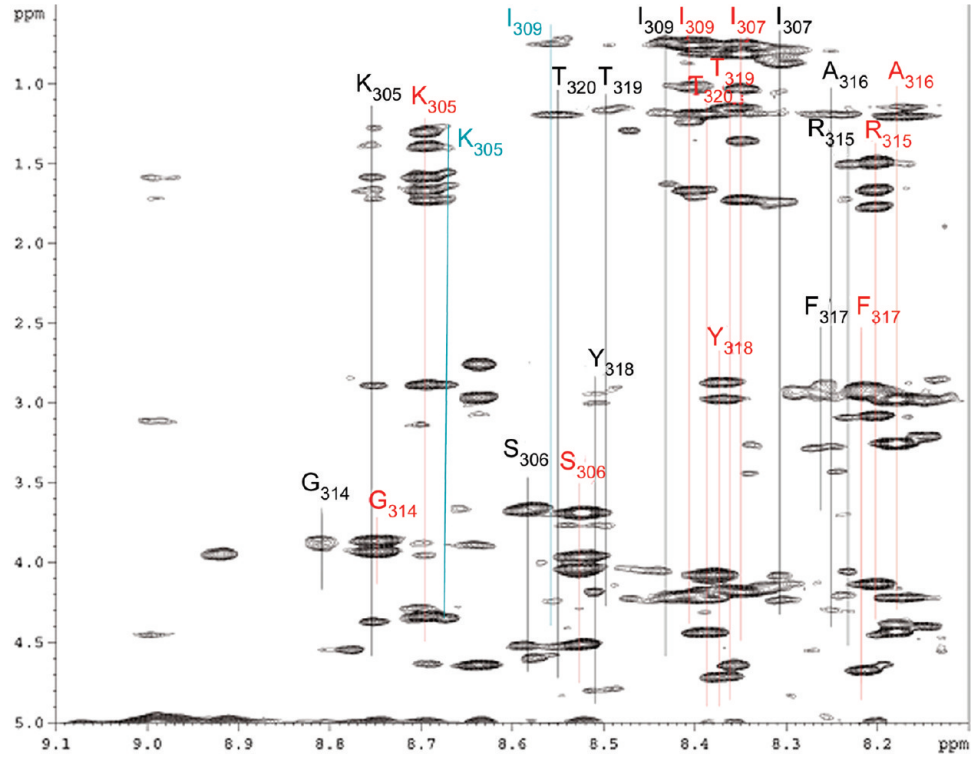

FIGURE 1: The HOHAHA spectrum of the $V3_{T303\text{-}E322}$ peptide. The spectral region showing amide proton interactions with Hα and nonaromatic side chain protons is shown. Line, letter, and number marked on the spectrum indicate the amide chemical-shift, residue name, and number, respectively. Different lines for the same residue present the multiple spin-systems. Color coding: red - dominant spin-system; black - secondary spin-system; turquoise - tertiary spin-system.

for its consistency with the manually assigned cross-peaks. The structure of the double constrained peptide $V3_{T303C\text{-}E322C;I309C\text{-}A316C}$ was calculated using the Crystallography and NMR System (CNS) program using the distance geometry-simulated annealing method, starting from extended conformation. After initial structure calculations, hydrogen bonds were identified using the program molmol and added as constraints to the structure calculation. The resulting 10 structures with the lowest energy were selected for structural statistics.

RESULTS

Peptide Design. The $V3_{IIIB}$ epitope recognized by the 0.5β antibody encompasses residues K305−I320 (16 residues) and the $V3_{MN}$ and $V3_{JR\text{-}FL}$ epitopes recognized by the 447−52D antibody include residues K305-T320 (14 residues) and R304-G321 (16 residues), respectively. The apparent disagreement between the epitope length of $V3_{MN}$ and $V3_{JR\text{-}FL}$ calculated on the basis of the numbering of the terminal residues and its actual length given in parentheses is due to the numbering of gp120 residues according to $gp120_{IIIB}$, which has a two-residue insertion, Q310-R311. In addition to residues 305−321, the structure of $V3_{JR\text{-}FL}$ bound to 447−52D includes E322 which was found to form electrostatic interactions with R304. This interaction could stabilize the β-hairpin conformation and dictate the pairing of the residues and, therefore, we have decided to include E322 in the peptides that we investigated. The sequence of the peptides is based on the $V3_{JR\text{-}FL}$ sequence which represents the consensus sequence of the clade-B R5 HIV-1 strains. The first peptide representing the V3-epitope of the HIV-1 neutralizing antibodies contained a disulfide bond between residues 303 and 323 that flank the segment R304-E322. For the other peptides, the location of the disulfide was moved systematically inward and as a result replacement of the epitope residues with cysteine was necessary. The peptide $V3_{K305C\text{-}T320C}$ was sparsely soluble and to increase its solubility, T303 and I323 were replaced by arginine.

In an attempt to stabilize the V3 β-hairpin we also replaced the L-proline in the GPGR segment by D-proline. For comparison with the constrained peptides, we included in this study a linear V3 peptide and a peptide consisting of the entire V3 sequence with a disulfide bond at its base. A list of all the peptides that were investigated by NMR is presented in Table 1. Our evaluation included one linear V3 peptide, six peptides constrained by one disulfide bond, one peptide constrained by the replacement of L-Pro with D-Pro, and two peptides constrained by two disulfide bonds.

Sequential Assignment of Peptides Constrained by a Single Disulfide Bond or D-Pro. The HOHAHA spectra indicate that conformational heterogeneity exists for all V3 peptides with a single disulfide bond except for $V3_{K305C\text{-}T320C}$ as judged by the appearance of multiple spin systems for some of the peptide residues. In all cases, a dominant spin-system from the major conformation could be identified (Figure 1). One explanation for the appearance of a second conformation is *cis*−*trans* isomerization around the peptide bond involving the nitrogen of P313. The ratio between the intensities of the multiple cross-peaks is approximately the ratio expected for the *trans* and *cis* isomers of proline (~4:1). Severe cross-peak overlap further complicated the sequential assignment procedure. Nevertheless, we have obtained 99%, 96.6%, 91.4%, 94%, and 94.5% of the assignments for the proton resonances of $V3_{T303C-I323C}$, $V3_{T303C\text{-}E322C}$, $V3_{R304C\text{-}G321C}$,

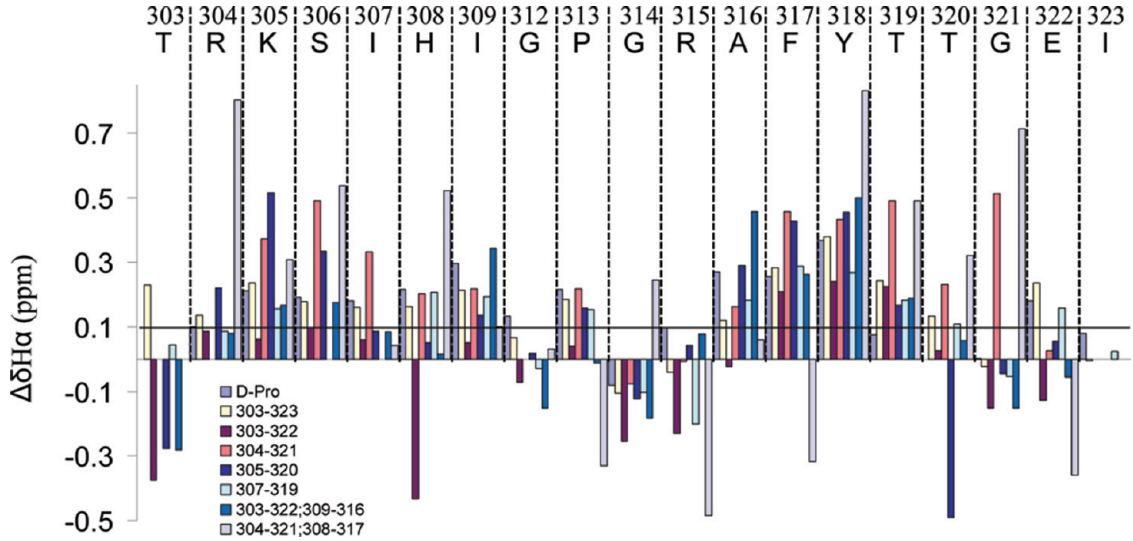

FIGURE 2: A histogram depicting the deviation of the H^{α} chemical shifts from their random coil values ($\Delta\delta H\alpha$) for each residue in the peptide $V3_{D\text{-}Pro}$, $V3_{T303C-I323C}$, $V3_{T303\text{-}E322}$, $V3_{R304C\text{-}G321C}$, $V3_{K305C\text{-}T320C}$, $V3_{I307C\text{-}T319C}$, $V3_{T303C\text{-}E322C;I309C\text{-}A316C}$, and $V3_{R304C\text{-}G321;H308C-F317C}$ (D-Pro, 303−323, 303−322, 304−321, 305−320, 307−319, 303−322; 309−316, 304−321; 308−317, respectively, in the color legend given inside the figure). The presented sequence in the top of the figure corresponds to the conserved sequence of the linear $V3_{JR\text{-}FL}$ peptide, with numbering according to HXB2 strain.

$V3_{K305C\text{-}T320C}$, and $V3_{I307C\text{-}T319C}$, respectively. For $V3_{D\text{-}Pro}$ 76% of the protons were assigned. No attempt to complete the assignment was made since its structure was not determined.

Hα Chemical Shift Deviations. The deviation of the Hα chemical shifts from their random coil values is a strong indicator for the secondary structure and the degree of population in helical and β-sheet conformation in peptides and proteins (*68*). Deviations greater than 0.1 ppm for three or more adjacent residues are consistent with a β-hairpin or β-sheet structure (*68*) and such deviations have been used to quantify the population of peptide residues in a β-hairpin conformation (*69*). For referencing purposes, linear peptides with L-proline at the turn were shown to be completely unfolded (*70*), while homologous cyclic peptides with D-Pro at the turn were assumed to be completely in a β-hairpin conformation (*69, 71*). Indeed, linear $V3_{MN}$ and $V3_{IIIB}$ peptides exhibited very small deviations of the Hα chemical shifts from their random coil values, indicating a random conformation for these unconstrained peptides (*10, 11*).

Examination of the deviation of the Hα chemical shifts from their random coil values ($\Delta\delta H\alpha$) reveals values >0.1 ppm for many residues in the constrained V3 peptides examined in the present study, indicating significant populations of β-strand conformations (Figure 2). The peptide $V3_{T303C-I323C}$ exhibits $\Delta\delta H\alpha$ deviations larger than 0.1 ppm for residues R304−I309 and for residues A316−T320 with an average of 0.204. In the peptide $V3_{T303C\text{-}E322C}$ only residues F317−T319 near the C-terminus exhibits deviations greater than 0.1 ppm indicating that this peptide is more flexible than $V3_{T303C-I323C}$. The peptide $V3_{R304C\text{-}G321C}$ exhibits $\Delta\delta H\alpha$ values larger than 0.1 ppm for segments K305−I309 and A316−C321 with an average of 0.355 for these residues and is the V3 peptide with one disulfide bond that exhibits the strongest tendency to adopt a β-hairpin conformation. In $V3_{K305C\text{-}T320C}$, residues R304−S306 and A316−T319 exhibit $\Delta\delta H\alpha$ larger than 0.1 ppm, indicating a significant population in an extended conformation. The peptides $V3_{I307C\text{-}T319C}$ and $V3_{D\text{-}Pro}$ reveal a similar tendency to form a β-hairpin. Residues K305, H308, and I309 and A316−T320 of $V3_{I307C\text{-}T319C}$ and K305−I309 and A316−T319 of $V3_{D\text{-}Pro}$ reveal $\Delta\delta H\alpha$ larger than 0.1 ppm with average values of 0.186 and 0.217 for $V3_{I307C\text{-}T319C}$ and $V3_{D\text{-}Pro}$, respectively, also indicating that there is a significant population in a β-hairpin conformation. The chemical shift deviation values observed for all of the V3 peptides constrained by one disulfide bond and $V3_{D\text{-}Pro}$ are on average significantly smaller than those observed for GB1 peptides that are constrained by both D-Pro and disulfide bond (*72*) indicating that despite their β-sheet propensities, the constrained V3 peptides have some residual flexibility.

Although no evidence for β-hairpin conformation has been reported for a 35-residue peptide comprising the entire V3 sequence with a disulfide bond at its base (*45*), we investigated the $V3_{JR\text{-}FL}$ peptide comprising the entire V3 sequence (data not shown). Except for F317 and Y318 which had $\Delta\delta H\alpha$ values greater than 0.1 ppm (0.116 and 0.202, respectively), we found that for the most part this peptide exhibits only small and random $\Delta\delta H\alpha$ deviations indicating a mostly random conformation.

Short Range Sequential NOE Interactions. Sequential nuclear Overhauser connectivities have been extensively used as qualitative indicators of peptide secondary structure (*73*). A diagram of the sequential connectivities of the peptides $V3_{T303C\text{-}E322C}$, $V3_{R304C\text{-}G321C}$, $V3_{K305C\text{-}T320C}$, and $V3_{I307C\text{-}T319C}$ is presented in Figure 3. Multiple $NN_{i,i+1}$ interactions accompanied by strong $\alpha N_{i,i+1}$ NOEs are indicative of disordered conformations, while the absence of, or the observation of, very weak $NN_{i,i+1}$ interactions in the presence of strong $\alpha N_{1,i+1}$ connectivities indicates a more extended strand conformation similar to a β-strand. All studied V3 peptides constrained by a single disulfide bond reveals strong $\alpha N_{i,i+1}$ NOEs. As for the $NN_{i,i+1}$ NOEs, the peptide $V3_{T303C\text{-}E323C}$ contains at least five $NN_{i,i+1}$ interactions (data not shown) and the peptide $V3_{T303C\text{-}E322C}$ reveals seven medium-weak $NN_{i,i+1}$ interactions (Figure 3A). The peptide $V3_{R304C\text{-}G321C}$ (Figure 3B) exhibits seven $NN_{i,i+1}$ interactions considerably weaker than those observed for $V3_{T303C\text{-}E322C}$ indicating decreased flexibility of the peptide $V3_{R304C\text{-}G321C}$ which was constrained to the X4 conformation of the V3.

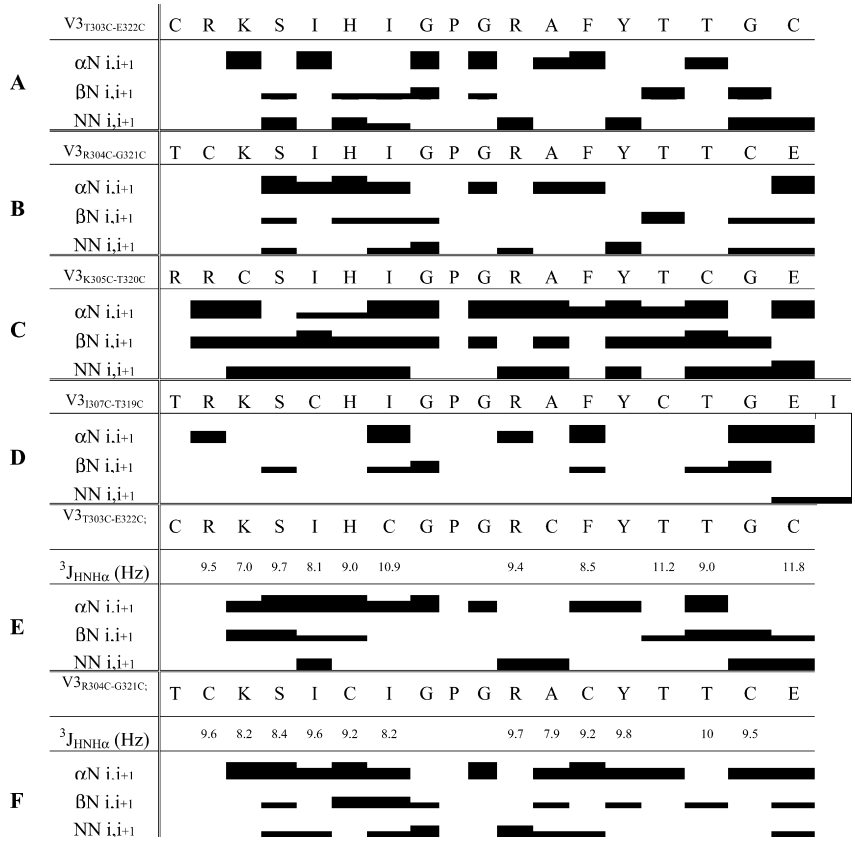

FIGURE 3: Summary of the sequential NOE interactions for $V3_{T303C\text{-}E322C}$ (A), $V3_{R304C\text{-}G321C}$ (B), $V3_{K305C\text{-}T320C}$ (C), $V3_{I307C\text{-}T319C}$ (D), $V3_{T303C\text{-}E322C;I309C\text{-}A316C}$ (E), and $V3_{R304C\text{-}G321C;H308C-F317C}$ (F). $^3J_{HNH\alpha}$ values are listed only for $V3_{T303C\text{-}E322C;I309C\text{-}A316C}$ and $V3_{R304C\text{-}G321C;H308C-F317C}$. Connectivities are derived from NOE assignment (and $^3J_{HNH\alpha}$ couplings from DQF-COSY) experiments. Filled boxes indicate the presence of sequential connectivity between the residue at the box position (i+1) with the proceeding residue (i). Box relative thickness indicates distance between interacting residues: thick box (<3 Å), medium (<4 Å), and thin (>4 Å).

The peptide $V3_{K305C\text{-}T320C}$ reveals 11 medium-weak $NN_{i,i+1}$ interactions (Figure 3C). Altogether, these data indicate the presence of conformational flexibility in all four peptides with more restricted flexibility for $V3_{R304C\text{-}G321C}$. On the other hand, only 2 $NN_{i,i+1}$ interactions (between G321 and E322 and E322 and I323) are observed for the peptide $V3_{I307C\text{-}T319C}$ in which the disulfide bond is closer to the GPGR segment (Figure 3D) indicating that this peptide shows a higher tendency to adopt an extended conformation resembling a β-strand conformation. The peptide $V3_{D\text{-}Pro}$ shows numerous $NN_{i,i+1}$ interactions with medium intensities indicating conformational flexibility also for this peptide (data not shown).

Medium- and Long-Range NOE Interactions in the Constrained Peptides. A necessary indicator for a β-hairpin formation is the detection of cross-strand interactions; long-range side chain−side chain, backbone−side chain and backbone−backbone interactions. In addition i,i+2 side chain−side chain interactions should be observed in each strand of the β-hairpin. We measured NOESY spectra for all peptides constrained by a single disulfide bond in H_2O and D_2O solutions and assigned the NOE cross-peaks to the corresponding interactions. To assess the influence of the disulfide bond on the V3 conformation, we compared the NOESY spectrum of the linear V3 peptide to those obtained for the constrained peptide. Initially, we concentrated on the section of the spectrum that shows interactions between aromatic protons and aliphatic side chain protons. As shown in Figure 4A, the linear $V3_{JR\text{-}FL}$ peptide does not exhibit any long-range interstrand NOE interactions, nor i,i+2 side chain-side chain interactions involving the aromatic protons of H308, F317, and Y318. On the other hand, as shown in Figure 4B, the entire cyclic-V3 peptide exhibits several weak long-range interactions involving the aromatic protons of F317 and Y318 with residues I307 and I309.

To investigate how the location of the disulfide bond influences the conformation of the V3 loop region, we examined the NOESY spectra of peptides $V3_{T303C-I323C}$, $V3_{T303C\text{-}E322C}$, $V3_{R304C\text{-}G321C}$, $V3_{K305C\text{-}T320C}$, and $V3_{I307C\text{-}T319C}$ in which the location of the disulfide bond was changed to give increasingly smaller rings (Table 1). As indicated in Figure 4C $V3_{T303C-I323C}$ exhibits several i,i+2 side chain NOE interactions characteristic of a β-hairpin conformation (F317/T319 and Y318/A316). In addition, long-range NOE interactions are observed among the side chains of I307 and/or I309 (the chemical shift of the methyl protons of I307 and I309 overlaps) at the N-terminal strand and the aromatic protons of both F317 and Y318 at the C-terminal strand.

The NOESY spectrum of $V3_{T303C\text{-}E322C}$ exhibits excellent signal-to-noise ratio and was studied in detail. Long range side chain−side chain interactions are observed between R304 and T319 and between S306 and T319 (Data not shown. All panels in Figure 4 show exclusively interactions between aromatic protons and both α and nonaromatic side-chain protons), the aromatic protons of both F317 and Y318 interact with the methyl protons of I309 (Figure 4D) and the side chain of H308 interacts with the side chains of Y318, and T320 (Figure 4D). Long range backbone−backbone

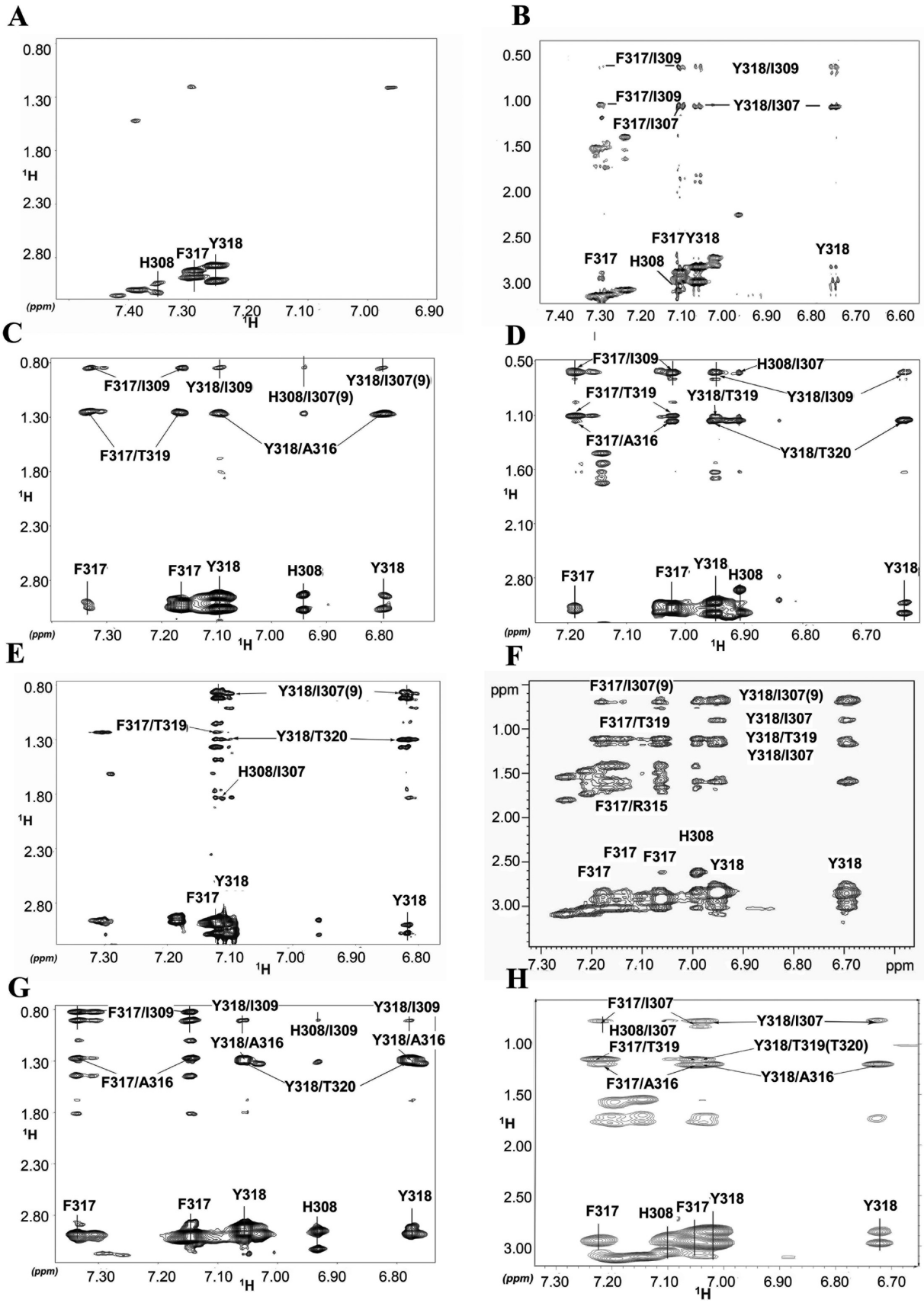

FIGURE 4: NOESY spectra presenting the interaction of aromatic protons with nonaromatic side chain protons: (A) unconstrained $V3_{JRFL}$, (B) entire V3, (C) $V3_{T303C-I323C}$, (D) $V3_{T303C-E322C}$, (E) $V3_{R304C-G321C}$, (F) $V3_{K305C-T320C}$, (G) $V3_{I307C-T319C}$, (H) V3 D-Pro. Assignment of cross-peaks representing interactions used in the analysis is shown.

interactions are observed between S306 and T319 and between H308 and T319 (data not shown). In addition, numerous long-range backbone−side chain interactions are observed as well between the N- and C-terminal strands (C303−I309 and A316−C322).

In addition to these long-range interactions, the peptide

$V3_{T303C\text{-}E322C}$ exhibits a combination of i,i+1 and i,i+2 side chain interactions (A316/F317, F317/T319, a weak Y318/T319 interaction and strong Y318/T320 as well as H308 with I307). Taken together with the fact that the long-range side chain interactions between the N- and C-terminal strands are between one residue on the N-terminal strand with two adjacent residues on the C-terminal strand or vice versa, the combination i,i+1 and i,i+2 side chain interactions indicate the existence of conformational flexibility and/or that the topology of the V3 chains in $V3_{T303C\text{-}E322C}$ is not that expected for a classic β-hairpin.

When the position of the N- and C-terminal terminal cysteines are moved one residue inward from 303 to 304 and from 322 to 321, the NOESY spectrum (Figure 4E) reveals the appearance of pairwise side chain−side chain interactions characteristic of a β-hairpin (F317/T319 and Y318/T320 shown in Figure 4E and K305/I307, not shown in the section presented). The peptide $V3_{R304C\text{-}G321C}$ also exhibits strong long-range NOE interactions between the aromatic protons of Y318 and the methyl protons of I307 and/or I309 (Figure 4E). No interaction could be observed between the aromatic protons of F317 and either I307 nor I309. The side chain of K305 interacted with the side chains of both Y318 and T320 (but not with T319 or C321). In addition several backbone−side chain interactions are observed between the segment K305−I309 and A316−320. However, no backbone−backbone interactions could be unambiguously assigned. Thus, unlike the previous two peptides, $V3_{T303C\text{-}E322C}$ and $V3_{T303C-I323C}$, the peptide $V3_{R304C\text{-}G321C}$ is less flexible and adopts a conformation more similar to a classical β-hairpin.

The NOESY spectrum of $V3_{K305C\text{-}T320C}$ exhibits strong NOE interactions between several side chain protons of I307 and I309 and the aromatic side chain of Y318 (Figure 4F). The methyl protons of I307 and I309 also interact with the aromatic side chain of F317; however, these interactions are considerably weaker in comparison with the interactions with Y318. The aromatic Y318 ring reveals weak interaction with side chain protons of C320 and T319. Side chain protons of F317 reveal strong or medium i,i+2 NOE interactions with side chain protons of R315 and T319. The aromatic F317 ring interacts also with side chain protons of S306 and H308. The long-range interactions and the i,i+2 side chain interactions indicate the existence of significant population in a β-hairpin; however, some conformational flexibility exists and it is possible that a subpopulation of molecules forms a hydrophobic cluster with F317 interacting with numerous N-terminal side chains.

The NOESY spectrum of $V3_{I307C\text{-}T319C}$ exhibits strong NOE interactions between F317 with both methyl groups of I309 (Figure 4G). The chemical shifts of the two methyl group are different, providing further evidence for decreased flexibility in this peptide. The dispersion of the aromatic protons of this peptide allowed us to detect an NOE interaction between the aromatic protons of Y318 and H308 (data not shown). Only very weak interactions are observed between the γ2 methyl protons of I309 and Y318. Multiple long-range side chain-backbone interactions are observed between the N- and C-terminal strand involving residues H308−G312 and A316−Y318. Several side chain i,i+2 NOE interactions are detected (A316/Y318, Y318/T320). Therefore, we conclude that the pattern of medium and long-range NOE interactions observed for $V3_{I307C\text{-}T319C}$ is characteristic of a β-hairpin conformation in the segment C307−C319, although definition of an ideal β-hairpin conformation requires the observation of additional long-range backbone−backbone interactions which are not detected or could not be unambiguously assigned. The presence of cross-peaks between the adjacent A316/F317 corresponds to the presence of a five residue GPGRA turn, as a result of which these side chains would be in proximity. No long-range interactions are observed between the N-terminal segment T303−S306 and the C-terminal segment T320−I323 indicating that these two segments are not part of the β-hairpin like conformation and that these two segments are rather flexible.

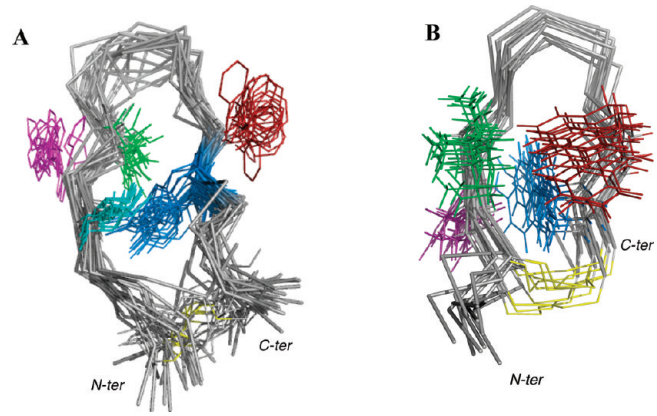

FIGURE 5: The Cα trace of the ten lowest-energy structures of $V3_{R304C\text{-}G321C}$ (A) and $V3_{I307C\text{-}T319C}$ (B). The disulfide bond is marked in yellow. Side-chains of the following residues are marked: H308-magenta; I309-green; F317-red; Y318-blue.

The NOESY spectrum of the peptide $V3_{D\text{-}Pro}$ manifests long-range side chain interactions indicating that the conformation of this peptide is constrained (Figure 4H). Both F317 and Y318 interact with the methyl protons of I307 and I309 (Figure 4G) and the corresponding cross-peaks have similar intensities indicating an equilibrium between multiple conformations some of which could resemble a β-hairpin or the formation of a hydrophobic core similar to a molten globule.

Structures of Peptide Constrained by a Single Disulfide Bond or D*-Pro.* Analysis of the NMR data indicates that the V3-peptides constrained by a single disulfide bond (except perhaps $V3_{T303C-I323C}$) have a conformational distribution with a significant population in a β-hairpin conformation. However, on the basis of the δHα deviations around 0.1−0.2 ppm and the coexistence of strong $\alpha N_{i,i+1}$ and medium weak $NN_{i,i+1}$ we conclude that $V3_{T303C-I323C}$, $V3_{T303C\text{-}E322C}$, $V3_{K305C\text{-}T320C}$, and $V3_{D\text{-}Pro}$ retain a significant degree of flexibility and cannot be represented by a single structure. On the other hand, the peptides $V3_{R304C\text{-}G321C}$ and $V3_{I307C\text{-}T319C}$ exhibited less flexibility in comparison with the other four peptides constrained by a single disulfide or by D-Pro and therefore their structures were determined. Our calculation of the structures of $V3_{R304C\text{-}G321C}$ and $V3_{I307C\text{-}T319C}$ used 191 and 221 NMR-derived constraints, respectively. Superposition of the lowest energy structures of $V3_{R304C\text{-}G321C}$ and $V3_{I307C\text{-}T319C}$ are shown in Figure 5. The average backbone rmsd's (for all residues between, and including, the two cysteine residues in each peptide) for the 20 lowest energy structures, to the mean coordinates of the

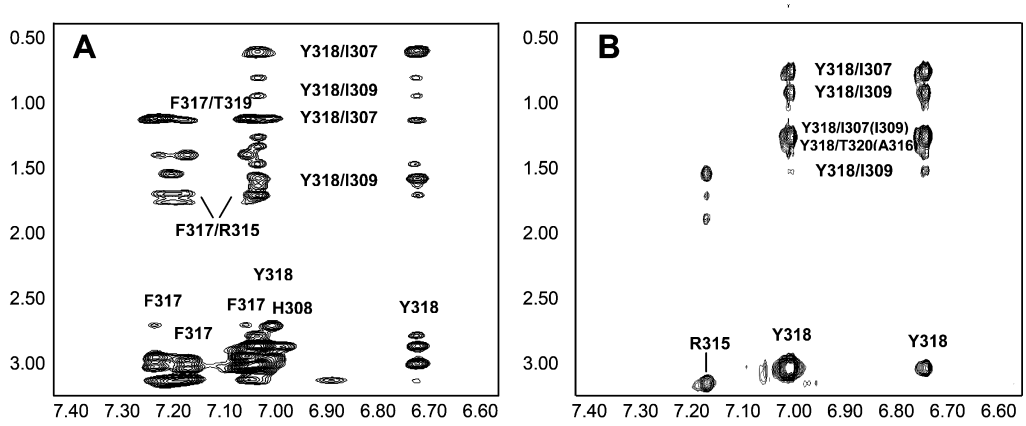

FIGURE 6: NOESY spectra of (A) $V3_{T303C\text{-}E322C;I309C\text{-}A316C}$ (B) $V3_{R304C\text{-}G321C;H308C-F317C}$. The section containing the interactions of the aromatic protons with nonaromatic side chain protons is presented. Assignment of cross-peaks representing interactions used in the analysis is shown.

output bundles, are 1.7 ± 0.5Å for $V3_{R304C\text{-}G321C}$ and 0.5 ± 0.17Å for $V3_{I307C\text{-}T319C}$. The calculated structures for the two peptides are similar to a β-hairpin. The structure of $V3_{R304C\text{-}G321C}$ peptide (Figure 5A) exhibits the characteristic organization of alternative side chains of the N- and C-terminal strands. Thus, a distinct pairing of residues is observed and side chains of every other residue point in the same direction creating one surface composed of the side chains of I307, I309, and Y318 and the opposite face formed by the side chains of H308 and F317. The structure of $V3_{I307C\text{-}T319C}$ (Figure 5B) also reveals characteristic features typical to a β-hairpin conformation but only in the segment C307−C319. The side chains of residues I309 and F317 point in one direction, while those of H308 and Y318 point in the other direction of the β-hairpin. The structure of the segments T303−S306 and T320−I323, which are outside the disulfide enclosed ring of $V3_{I307C\text{-}T319C}$, could not be defined due to their flexibility.

NMR Characteristics of Peptides with Two Disulfide Bonds. Two peptides, $V3_{T303C\text{-}E322C;I309C\text{-}A316C}$ and $V3_{R304C\text{-}G321C;H308C-F317C}$, each constrained by two disulfide bonds were studied by NMR. A nearly complete proton resonance assignment has been achieved for both peptides. The sequential connectivities of $V3_{T303C\text{-}E322C;I309C\text{-}A316C}$ and $V3_{R304C\text{-}G321C;H308C-F317C}$, and the $^3J_{HNH\alpha}$ coupling constants are presented in Figure 3, panels E and F, respectively. Eleven $^3J_{HNH\alpha}$ values could be determined for $V3_{T303C\text{-}E322C;I309C\text{-}A316C}$ and all except one are characteristic of a β-strand conformation. Twelve $^3J_{HNH\alpha}$ coupling were determined for $V3_{R304C\text{-}G321C;H308C-F317C}$ and they range between 7.9 to 10 Hz indicating that the majority of these peptide molecules populate a β-hairpin conformation.

Examination of the deviation of the Hα chemical shifts from their random coil values, $\Delta\delta H\alpha$, of the two peptides (Figure 2) reveals that residues K305, S306, C309, and C316−T319 of $V3_{T303C\text{-}E322C;I309C\text{-}A316C}$ and C304−S306, H308, I309 and Y318−C321 of $V3_{R304C\text{-}G321C;H308C-F317C}$ exhibit $\Delta H\alpha$ greater than 0.1 ppm. The average of ΔδHα for those residues exhibiting ΔδHα values greater than 0.1 ppm increases from 0.225 for $V3_{T303C\text{-}E322C}$ to 0.292 for $V3_{T303C\text{-}E322C;I309C\text{-}A316C}$ and from 0.355 for $V3_{R304C\text{-}G321C}$ to 0.566 for $V3_{R304C\text{-}G321C;H308C-F317C}$. This comparison is consistent with a slight increase in β-strand conformational stability for $V3_{T303C\text{-}E322C;I309C\text{-}A316C}$ in comparison with $V3_{T303C\text{-}E322C}$ and considerable increase in β-strand conformational stability for $V3_{R304C\text{-}G321C;H308C-F317C}$ in comparison with $V3_{R304C\text{-}G321C}$. The unexpected low values of ΔδHα observed for H308 in $V3_{T303C\text{-}E322C;I309C\text{-}A316C}$ and I307 in $V3_{R304C\text{-}G321C;H308C-F317C}$ can be explained by cross-strand interaction with aromatic residues and a concomitant ring current effect on the chemical shift.

The NOESY spectrum of $V3_{T303C\text{-}E322C;I309C\text{-}A316C}$ peptide (Figure 6A) shows the following cross-strand NOE interactions: I307/C316, I307/Y318, S306/Y318, F317/H308, K305/Y318, and K305/T319. Numerous backbone-side chain interactions are observed between the N- and C- terminal strands. Backbone−backbone NOEs are observed between I307 and Y318, H308 and F317, G312 and R315 and between G312 and C316. Side chain−side chain interactions between residues i,i+2 indicative of a β-hairpin conformation are also observed in each of the strands (K305/I307, I307/C309, C316/Y318, and T319/G321) (Only interactions between aromatic protons and nonaromatic side chain protons as well as α protons are shown in Figure 6A and B). It should be emphasized that while the aromatic protons of Y318 interact with the methyl protons of I307, no side chain interactions between the aromatic protons of F317 with I307 were observed indicating that the peptide $V3_{T303C\text{-}E322C;I309C\text{-}A316C}$ is considerably less flexible than all the V3 peptides constrained by a single disulfide bond to the R5 V3 conformation.

The NOE interactions observed for the peptide $V3_{R304C\text{-}G321C;H308C-F317C}$ indicate that this peptide formed a structure that was closest to a typical β-hairpin conformation. Numerous side chain−side chain interactions characteristic of a β-hairpin conformation are observed between I309 and Y318, I307 and Y318, I307 and T320, S306 and C317, S306 and T319 and C304 and T319 (all interactions involving aromatic residues are shown in Figure 6B). Long-range backbone−backbone NOE interactions are observed between I307 and C317, C308 and C317, C308 and Y318, I307 and Y318, K305 and C321, and C304 and C321 (data not shown). In addition numerous long-range side chain−backbone interactions between the N- and C-terminal strands are observed. In addition i,i+2 side chain-side chain interactions are observed between I307 and I309, A316 and Y318 and between Y318 and T320. Two NOE interactions between Pro312 H^{α}/Gly314 H^{N} and Pro312 H^{α}/Arg315 H^{N} define the loop-region conformation. Pro312 is found in a *trans* isomer configuration as supported by the presence of strong NOE

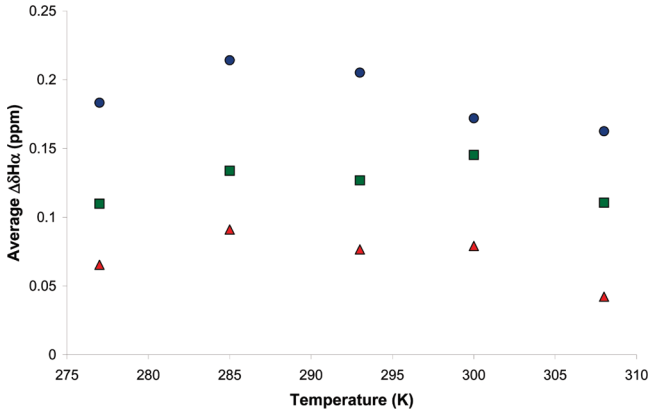

FIGURE 7: Temperature dependence of $\Delta\delta H^{\alpha}$ averaged for all peptide residues. The average was calculated for the entire peptide sequence excluding the 312GPGR^{315} segment and residues for which an assignment was not available. Red triangles- $V3_{T303C\text{-}E322C}$; green squares - $V3_{T303C\text{-}E322C;I309C\text{-}A316}$; blue circles- $V3_{R304C\text{-}G321C}$.

interactions between Gly311 H^{α}/Pro312 H^{Δ}, which are characteristic for this isomer.

Calculation of Temperature Coefficients. Using HOHAHA spectra acquired at various temperatures, we calculated the temperature coefficients of the backbone amide protons $d(\delta H^{N})/dT$ [ppb/K] for four representative peptides. These coefficients are valuable probes for the degree of protection of such nuclei from solvent exchange (*74*). An amide NH temperature coefficient more positive than −4.5 ppb/K indicates relative solvent inaccessibility, probably due to involvement in hydrogen-bonding (*75*). In agreement with the high flexibilities we observed (vide supra), for $V3_{T303C\text{-}E322C}$, $V3_{T303C\text{-}E322C;I309C\text{-}A316C}$, and $V3_{R304C\text{-}G321C}$, these peptides did not have any residue with a temperature coefficient more positive than the threshold −4.5 ppb/K (data not shown). This suggests that no hydrogen-bonds in these peptides could be inferred from the temperature coefficient data. However, the amide protons of residues R315 and Y318 of the $V3_{R304C\text{-}G321C;H308C-F317C}$ peptide have temperature coefficients indicative of solvent protection (−3.95 and −3.1 ppb/K, respectively), therefore implying the involvement of these backbone atoms in hydrogen bonding.

Temperature Stability of the β-Hairpin Conformation. As mentioned above, the values of $\Delta\delta H^{\alpha}$ can give quantitative measure of the population in a β-hairpin conformation. To learn about the temperature stability of the β-hairpin conformation in the constrained V3 peptides we measured $\Delta\delta H^{\alpha}$ for the three representative constrained V3 peptides $V3_{T303C\text{-}E322C}$, $V3_{T303C\text{-}E322C;I309C\text{-}A316C}$, and $V3_{R304C\text{-}G321C}$ at different temperatures. The average $\Delta\delta H^{\alpha}$ values for all peptide residues in the β-strand flanked by the cysteines were calculated as a function of temperature. The average did not include residues 303 and 304 for which we did not obtain H^{α} assignment or residues G312−R315 that are thought to constitute the turn. The peptides $V3_{T303C\text{-}E322C}$ and $V3_{T303C\text{-}E322C;I309C\text{-}A316C}$ show no significant changes in the average $\Delta\delta H^{\alpha}$ as a function of the temperature (Figure 7) and maintained a relatively low average $\Delta\delta H^{\alpha}$ (0.05−0.13 ppm) over all temperatures, indicating that these peptides have only a small population in a β-hairpin conformation. In contrast $V3_{R304C\text{-}G321C}$ had average $\Delta\delta H^{\alpha}$ values close to 0.2 ppm and its β-hairpin conformation, based on changes in the average $\Delta\delta H^{\alpha}$, was somewhat more stable at 285 K. This single disulfide constrained peptide showed a typical thermodynamic signature of a folded β-structure with minor "cold" denaturation at 278 K and indication for "hot" denaturation for temperatures above 285 K. The relatively flat curve for $\Delta\delta H\alpha$ as a function of temperature suggests that although the NMR measurements have been carried out at 0.5 °C the β-hairpin exhibits only a minor decrease in stability at nearly physiological temperatures.

Structure Determination. The structure of $V3_{T303C\text{-}E322C;I309C\text{-}A316C}$ (Figure 8A,B) was determined on the basis of 191 constraints, 51 of which were medium and long-range (Table 3). The segments I307−C309 and C316−Y318 formed β-strands, while the segments C303−S306 and T319−C322 of $V3_{T303C\text{-}E322C;I309C\text{-}A316C}$ did not form a well-defined secondary structure. The segment G312−R315 forms a type IV β-turn. The average rmsd is 1.9 Å for all backbone atoms.

The structure of $V3_{R304C\text{-}G321C;H308C-F317C}$ (Figure 8C,D) was determined on the basis of 192 NOE constraints of which 86 are medium and long-range (Table 3). The ribbon representation structure is shown in Figure 8D. $V3_{R304C\text{-}G321C;H308C-F317C}$ forms a β-hairpin consisting of two antiparallel β-strands between residues C304−C308 and C317−C321. The side chains of K305, I307, I309, A316, Y318, and T320 form one face of the β-hairpin, while side chains of C304, S306, C308, C317, T319, and C321 form the other β-hairpin face. The segment G312−R315 forms a type IV β-turn. The Ramachandran plot reveals that about 83% of the residues (excluding Gly and Pro) are in the "most favored" regions of the plot, while the remaining 17% are in the "additionally allowed" regions (not shown).

Structural Comparison of Constrained V3 Peptides with Antibody Bound Peptides. Peptides $V3_{R304C\text{-}G321C}$ and $V3_{I307C\text{-}T319C}$ were designed to assume structures that should mimic the X4 and R5B conformations of the V3 loop, respectively. The comparison between the structure of the constrained peptide and the antibody-bound structures is presented in Figure 9A,B, respectively. Superposition of the structure of the segments K305−I309 and A316−T320 of the peptide $V3_{R304C\text{-}G321C}$ over the corresponding segments in the structure of a $V3_{IIIB}$ peptide bound to the 0.5β antibody (an X4 structure) (Figure 9A) (*19*) reveals a backbone rmsd value of 2.6 Å between the two structures. Comparison of the segments C307−I309 and A316−C319 in $V3_{I307C\text{-}T319C}$ over the corresponding segments of $V3_{JR\text{-}FL}$ peptide bound to 447−52D (an R5B structures) reveals an rmsd of 2.1 Å (Figure 9B). Comparison with antibody bound conformation of the V3 was done also for the two peptides constrained by two disulfide bonds. Overlay of the K305−T320 segment of $V3_{T303C\text{-}E322C;I309C\text{-}A316C}$ constrained to the R5A conformation of the V3 with the structure of $V3_{MN}$ bound to 447−52D (a R5A structure (*17*)) reveals considerable similarity between the two structures with an rmsd of 1.8 Å when the GPGR segment is included and an rmsd of 1.7 Å when the GPGR segment is excluded from the comparison (Figure 9C). The structure of $V3_{T303C\text{-}E322C;I309C\text{-}A316C}$ is less similar to that $V3_{JR\text{-}FL}$ bound to 447−52D (*21*) and $V3_{IIIB}$ bound to 0.5β (*19*) with backbone RMSDs of 2.15 and 2.9 Å, respectively. The structure of $V3_{R304C\text{-}G321C;H308C-F317C}$ constrained to the X4 conformation of the V3 is very similar to that of a $V3_{IIIB}$ peptide bound to the 0.5β antibody (*19*) with rmsd of 1.4 Å when the segments R304-I309 and A316-G321 of

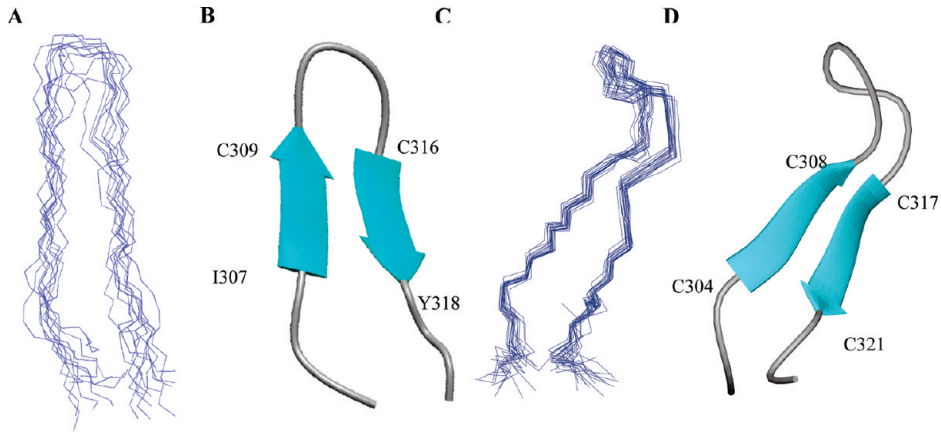

FIGURE 8: Backbone representation of the lowest energy solution structure and a ribbon diagram of $V3_{T303C\text{-}E322C;I309C\text{-}A316C}$ (A) and (B) and $V3_{R304C\text{-}G321C;H308C-F317C}$ (C) and (D), respectively.

Table 3: Experimental NMR Data and Structural Statistics of $V3_{T303C\text{-}E322C;I309C\text{-}A316C}$ and $V3_{R304C\text{-}G321C;H308C-F317C}$

	$V3_{T303C\text{-}E322C;I309C\text{-}A316C}$	$V3_{R304C\text{-}G321C;H308C-F317C}$
NMR distance constraints		
total	191	192
medium and long-range	51	86
torsion angle	11	12
hydrogen bond	2	2
mean rmsd values, Å		
all backbone atoms	1.54	0.69 ± 0.20
all heavy atoms	2.24	0.92 ± 0.19
NOE violation		
max individual violation (Å)	0.5	
rmsd of NOE violation	0.024 ± 0.009	
deviation from ideal covalent geometry		
bond length (Å)	0.0008 ± 0.0001	
bond angles (°)	0.323 ± 0.003	
improper angles	0.089 ± 0.005	
distance constraint violoation[a]		
no. > 0.1 Å		5 ± 1
maximum (Å)		0.22 ± 0.03
torsion angle violation[a]		
no. > 5°		0
maximum (deg)		0.78 ± 0.32

[a] The values given are the average and the standard deviation over the 20 energy-minimized conformers with the lowest residual CYANA target function values that represent the NMR solution structure.

$V3_{R304C\text{-}G321C;H308C-F317C}$ are superimposed on the corresponding segments in the antibody-bound peptide (Figure 9D). The structure of $V3_{R304C\text{-}G321C;H308C-F317C}$ is very different from that of a $V3_{IIIB}$ bound to 447−52D (*20*) with backbone rmsd of 4.1 Å when the GPGR segment is included and 2.7 Å when the GPGR segment is excluded.

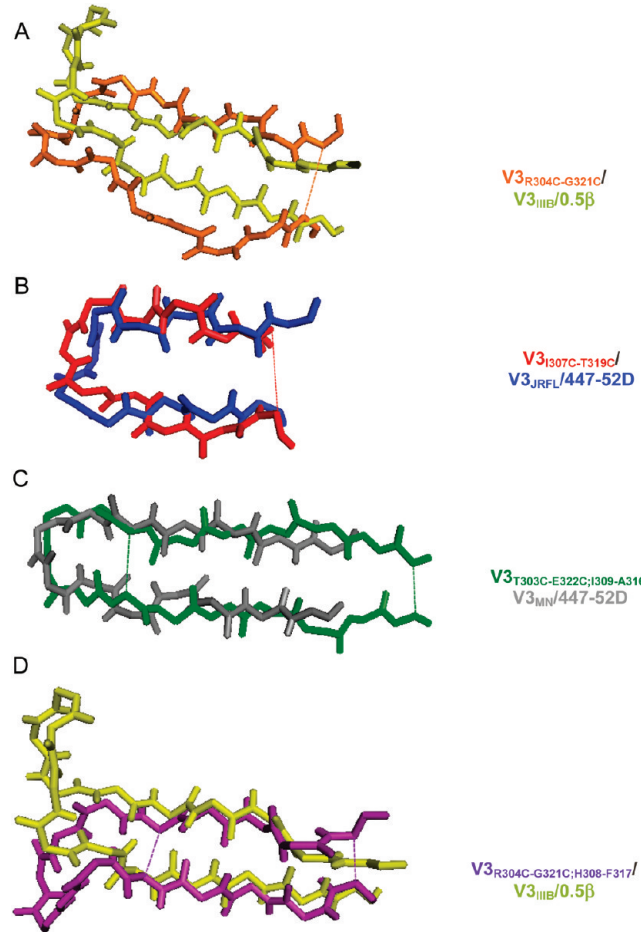

FIGURE 9: Backbone superposition of the NMR-derived solution structures of (A) $V3_{R304C\text{-}G321C}$ (orange) and the structure of $V3_{IIIB}$ in complex with the 0.5β Fv (yellow) (B) $V3_{I307C\text{-}T319C}$ (red) and the structure of $V3_{JRFL}$ in complex with Fv of 447−52D Ab (blue) (C) $V3_{T303C\text{-}E322C;I309\text{-}A316}$ (green) and the structure of $V3_{MN}$ in complex with Fv of 447−52D Ab (gray) and (D) $V3_{R304C\text{-}G321C;H308-F317}$ (purple) and the structure of $V3_{IIIB}$ in complex with the 0.5β Fv (yellow). Dashed lines indicate location of disulfide bonds.

DISCUSSION

In this study we have attempted to systematically constrain the conformations of V3 peptides to β-hairpin structures recognized by the 0.5β (postulated X4 V3 conformation) and 447−52D antibodies (postulated R5A and R5B V3 conformations). For this purpose we inserted one or two disulfide bonds at specific residues in a $V3_{JFRL}$ peptide sequence or replaced L-Pro with D-Pro to stabilize the turn of the β-hairpin. The NMR studies of these V3-analogs, and comparison with a linear V3 peptide and a cyclic V3 peptide comprising the entire V3 region provide supporting evidence that the constrained peptides assume β-hairpin-like conformations although in most cases an ideal β-hairpin conformation was not obtained. Linear V3 peptides do not show any long-range, cross-strand interactions and the deviations of the Hα chemical shift from their random coil values indicate

that there is no significant population in a β-hairpin conformation (*10, 11*). It has been reported that even cyclic 35-residue V3 peptides with a disulfide bond at the base do not exhibit long-range interactions and that their structure is flexible (*46, 76*). In the present study, we found only a few weak long-range interactions in the 35-residue cyclic V3 peptide and the $\delta H\alpha$ values were, for the most part, indicative of a random conformation. In contrast, we observed several long-range interactions especially between the aromatic residues of the C-terminal strand and the methyl protons of the isoleucine residues at the N-terminal strand in our constrained V3 peptides in which the disulfide bond was inserted closer to the tip of the β-hairpin. These long-range NOEs were accompanied by significant positive deviations of $\Delta\delta H\alpha$ values, and the $\alpha N_{i,i+1}$ sequential NOE interactions were considerably stronger than the observed $NN_{i,i+1}$ interactions. All of the NMR parameters thus support a β-hairpin structure as a significant contribution to the conformational distribution of many of the constrained V3-peptides. However, despite the covalent constraint of the peptides, significant residual flexibility was observed. In most of the peptides constrained by a single disulfide bond or D-Pro both F317 and Y318 interacted with the methyl protons of I307 and/or I309 indicating conformational flexibility with possible equilibrium between two β-hairpin conformations differing in the pairing of the residues and/or significant deviation from ideal β-hairpin conformation. While these interactions are comparable in intensity for $V3_{T303C,I323C}$, significant differences in intensity were observed for all other peptides indicating more restricted flexibility and increased similarity to an ideal and single β-hairpin conformation.

Of the peptides we studied, two, $V3_{R304C\text{-}G321C}$ and $V3_{R304C\text{-}G321C;H308C-F317C}$, were designed to mimic the X4 conformation. All NMR parameters indicate that it was easier to constrain the $V3_{JR\text{-}FL}$ epitope to the X4 conformation than to the R5 conformation using a single disulfide bond. According to the $\Delta\delta H\alpha$, $V3_{R304C\text{-}G321C}$ exhibited the most β-hairpin-like conformation in comparison with all peptides constrained by a single disulfide bond to mimic the R5 conformation except $V3_{I307C\text{-}T319C}$. Considering the long-range NOEs and the i,i+2 side chain NOES, $V3_{R304C\text{-}G321C}$ and $V3_{I307C\text{-}T319C}$ (constrained to the R5B conformation) have similar propensities to form β-hairpin conformations. This is despite the fact that the first has a ring size of 16 residues and the second has a ring size of 11 residues, which was the smallest ring size of all of the peptides constrained by a single disulfide examined by NMR in this study. The peptide $V3_{R304C\text{-}G321C;H308C-F317C}$, constrained by two disulfide bonds to mimic the X4 V3 conformation, has a striking similarity to the 0.5β antibody bound peptide with a backbone rmsd of 1.4 Å. Thus, this highly constrained peptide achieved the structure that it was designed to mimic.

In contrast to the X4 peptide designs, all peptides constrained by a single disulfide to assume the R5A or the R5B conformations exhibited appreciable conformational flexibility except for $V3_{I307C\text{-}T319C}$ which had the shortest ring size. Comparison of the $\Delta\delta H\alpha$ values reveals that $V3_{T303C,I323C}$ (constrained to the R5B conformation) has a stronger tendency to form a β-hairpin-like structure in comparison with $V3_{T303C,E322C}$ (constrained to the R5A conformation) despite the one residue longer ring size of the former. It could be that the R5B conformation is stabilized by an electrostatic interaction between R304 and E322 and therefore is easier to constrain by disulfide bond formation in comparison with the R5A conformation. Consistent with our design $V3_{I307C\text{-}T319C}$ (constrained to the R5B conformation) exhibited strong NOE interaction between the aromatic protons of F317 and the methyl protons of I309, and only weak interactions have been observed between Y318 and I309. On the basis of these NOEs and of all the accumulated NMR data, we conclude that of those peptides constrained by a single disulfide bond to assume R5-like structures $V3_{I307C\text{-}T319C}$ has the highest tendency to form a β-hairpin. However, since the strands outside the ring, that is, R304-S306 and T320-E322 are very flexible, unlike their extended conformation in $V3_{JR\text{-}FL}$ peptide bound to 447−52D (*21*), it is questionable whether this peptide will be a good immunogen for eliciting 447−52D-like antibodies.

The incorporation of a second disulfide bond into $V3_{JFRL}$ peptides increased the tendency of the V3 region to form a β-hairpin conformation. This is evidenced by the observation of several backbone−backbone interactions for both $V3_{T303C\text{-}E322C;I309C\text{-}A316C}$ and $V3_{R304C\text{-}G321C;H308C-F317C}$. As judged by the change in the $\Delta\delta H\alpha$ values of $V3_{T303C\text{-}E322C;I309C\text{-}A316C}$ in comparison to those of $V3_{T303C\text{-}E322C}$ the second constraint leads to some increase in β-hairpin stability. Indeed, the second constraint in $V3_{T303C\text{-}E322C;I309C\text{-}A316C}$ leads to formation of β-strands by I307−C309 and C316−Y318. However, six of the residues in the rings enclosed by the disulfide bonds, namely, C303−S306 and T319−C322, did not form an ideal β-strand. This is probably due to the five residue separation between the two disulfide bonds and the presence of a glycine residue in the C-terminal strand preceding C322. Nevertheless when compared to the conformation of $V3_{MN}$ peptide bound to 447−52D (*17*), $V3_{T303C\text{-}E322C;I309C\text{-}A316C}$ is an excellent mimic of the R5A conformation of the V3 epitope with a backbone rmsd of 1.8 Å. As summarized above, $V3_{R304C\text{-}G321C;H308C-F317C}$ exhibited even greater similarity to the X4-antibody-bound V3-conformation with a considerable increase in $\Delta\delta H\alpha$ values and the number of *J*-coupling values greater than 7.5 Hz in comparison with $V3_{R304C\text{-}G321C}$. Thus the smaller ring sizes in $V3_{R304C\text{-}G321C;H308C-F317C}$ result in a nearly ideal β-hairpin within the two rings formed by the disulfide bond (Figure 9D).

β-Hairpins contain hydrogen bond networks and these networks are critical for both stabilizing the bound V3 structures and its interactions with the 0.5β and 447−52D. The network of the hydrogen bonds in the structures of $V3_{T303C\text{-}E322C;I309C\text{-}A316C}$ and $V3_{R304C\text{-}G321C;H308C-F317C}$ determined in this study is as predicted on the basis of the location of the disulfide bonds in these two peptides. Thus these two structures unequivocally demonstrate that the location of the disulfide bond not only determines the pairing of the residues in the β-hairpin but also determines the hydrogen bond network. As expected, we also found that when $V3_{JF\text{-}RL}$ was constrained by single disulfide bonds the hydrogen bond network was less structured due to the overall increase in peptide flexibility.

Although increased rigidification and a greater tendency to form a β-hairpin conformation can be achieved by two disulfide bonds, this strategy requires the replacement of critical V3 residues with cysteine. The replacement of K305, I307, or I309 is required to obtain the R5 conformation of the V3. However, these residues were found to interact

strongly with 447−52D and their replacement in the immunogen may hamper the elicitation of antibodies cross-reactive with gp120. Therefore, although the doubly constrained peptides are more rigid and more similar in their conformation to an ideal β-hairpin, our study suggests that peptides constrained by one disulfide bond at the base of the V3 epitope recognized by 447−52D will be more attractive candidates for immunogens that elicit antibodies that neutralize HIV-1.

In conclusion, our NMR analysis provides evidence that disulfide bond constraints within the V3 epitope that is recognized by 447−52D can result in a markedly narrower conformational distribution of this molecule in solution and similarity to a β-hairpin conformation. The design we used resulted in several peptides that achieved conformations that were close to that of the presumed X4 conformation bound to the 0.5β antibody. More difficulty was encountered in designing peptides with R5-like structures. Although a disulfide bond close to the GPGR segment resulted in a conformation similar to the postulated R5B conformation of the V3, the strands outside the ring enclosed by the disulfide link are flexible limiting the utility of this constrained peptide. Incorporation of a second disulfide bond increases the rigidification and when the disulfide bonds are separated by three residues on each strand, the chains form a nearly ideal β-strand. However, the incorporation of two disulfide bonds requires the replacement of residues involved in extensive interactions with the antibodies, which may limit the utility of this strategy.

ACKNOWLEDGMENT

We thank Mr. Yehezkiel Hayek for excellent technical assistance in peptide purification.

REFERENCES

1. Rusche, J. R., Javaherian, K., McDanal, C., Petro, J., Lynn, D. L., Grimaila, R., Langlois, A., Gallo, R. C., Arthur, L. O., Fischinger, P. J., et al. (1988) Antibodies that inhibit fusion of human immunodeficiency virus-infected cells bind a 24-amino acid sequence of the viral envelope, gp120. *Proc. Natl. Acad. Sci. U. S. A. 85*, 3198–3202.
2. Wu, L., Gerard, N. P., Wyatt, R., Choe, H., Parolin, C., Ruffing, N., Borsetti, A., Cardoso, A. A., Desjardin, E., Newman, W., Gerard, C., and Sodroski, J. (1996) CD4-induced interaction of primary HIV-1 gp120 glycoproteins with the chemokine receptor CCR-5. *Nature (London) 384*, 179–183.
3. Trkola, A., Dragic, T., Arthos, J., Binley, J. M., Olson, W. C., Allaway, G. P., Cheng-Mayer, C., Robinson, J., Maddon, P. J., and Moore, J. P. (1996) CD4-dependent, antibody-sensitive interactions between HIV-1 and its co-receptor CCR-5. *Nature (London) 384*, 184–187.
4. Liao, H. X., Etemad-Moghadam, B., Montefiori, D. C., Sun, Y., Sodroski, J., Scearce, R. M., Doms, R. W., Thomasch, J. R., Robinson, S., Letvin, N. L., and Haynes, B. F. (2000) Induction of antibodies in guinea pigs and rhesus monkeys against the human immunodeficiency virus type 1 envelope: neutralization of nonpathogenic and pathogenic primary isolate simian/human immunodeficiency virus strains. *J. Virol. 74*, 254–263.
5. Letvin, N. L., Robinson, S., Rohne, D., Axthelm, M. K., Fanton, J. W., Bilska, M., Palker, T. J., Liao, H. X., Haynes, B. F., and Montefiori, D. C. (2001) Vaccine-elicited V3 loop-specific antibodies in rhesus monkeys and control of a simian-human immunodeficiency virus expressing a primary patient human immunodeficiency virus type 1 isolate envelope. *J. Virol. 75*, 4165–4175.
6. Someya, K., Cecilia, D., Ami, Y., Nakasone, T., Matsuo, K., Burda, S., Yamamoto, H., Yoshino, N., Kaizu, M., Ando, S., Okuda, K., Zolla-Pazner, S., Yamazaki, S., Yamamoto, N., and Honda, M. (2005) Vaccination of rhesus macaques with recombinant *Mycobacterium bovis* bacillus Calmette-Guerin Env V3 elicits neutralizing antibody-mediated protection against simian-human immunodeficiency virus with a homologous but not a heterologous V3 motif. *J. Virol. 79*, 1452–1462.
7. Hewer, R., and Meyer, D. (2005) Evaluation of a synthetic vaccine construct as antigen for the detection of HIV-induced humoral responses. *Vaccine 23*, 2164–2167.
8. Golding, B., Eller, N., Levy, L., Beining, P., Inman, J., Matthews, N., Scott, D. E., and Golding, H. (2002) Mucosal immunity in mice immunized with HIV-1 peptide conjugated to Brucella abortus. *Vaccine 20*, 1445–1450.
9. Haynes, B. F., Ma, B., Montefiori, D. C., Wrin, T., Petropoulos, C. J., Sutherland, L. L., Scearce, R. M., Denton, C., Xia, S. M., Korber, B. T., and Liao, H. X. (2006) Analysis of HIV-1 subtype B third variable region peptide motifs for induction of neutralizing antibodies against HIV-1 primary isolates. *Virology 345*, 44–55.
10. Zvi, A., Hiller, R., and Anglister, J. (1992) Solution conformation of a peptide corresponding to the principal neutralizing determinant of HIV-1IIIB: a two-dimensional NMR study. *Biochemistry 31*, 6972–6979.
11. Chandrasekhar, K., Profy, A. T., and Dyson, H. J. (1991) Solution conformational preferences of immunogenic peptides derived from the principal neutralizing determinant of the HIV-1 envelope glycoprotein gp120. *Biochemistry 30*, 9187–9194.
12. Sharon, M., Rosen, O., and Anglister, J. (2005) NMR studies of V3 peptide complexes with antibodies suggest a mechanism for HIV-1 co-receptor selectivity. *Curr. Opin. Drug Discovery Dev. 8*, 601–612.
13. Matsushita, S., Robert Guroff, M., Rusche, J., Koito, A., Hattori, T., Hoshino, H., Javaherian, K., Takatsuki, K., and Putney, S. (1988) Characterization of a human immunodeficiency virus neutralizing monoclonal antibody and mapping of the neutralizing epitope. *J. Virol. 62*, 2107–2114.
14. Gorny, M. K., Xu, J. Y., Karwowska, S., Buchbinder, A., and Zolla-Pazner, S. (1993) Repertoire of neutralizing human monoclonal antibodies specific for the V3 domain of HIV-1 gp120. *J. Immunol. 150*, 635–643.
15. Gorny, M. K., Revesz, K., Williams, C., Volsky, B., Louder, M. K., Anyangwe, C. A., Krachmarov, C., Kayman, S. C., Pinter, A., Nadas, A., Nyambi, P. N., Mascola, J. R., and Zolla-Pazner, S. (2004) The v3 loop is accessible on the surface of most human immunodeficiency virus type 1 primary isolates and serves as a neutralization epitope. *J. Virol. 78*, 2394–2404.
16. Binley, J. M., Wrin, T., Korber, B., Zwick, M. B., Wang, M., Chappey, C., Stiegler, G., Kunert, R., Zolla-Pazner, S., Katinger, H., Petropoulos, C. J., and Burton, D. R. (2004) Comprehensive cross-clade neutralization analysis of a panel of anti-human immunodeficiency virus type 1 monoclonal antibodies. *J. Virol. 78*, 13232–13252.
17. Sharon, M., Kessler, N., Levy, R., Zolla-Pazner, S., Gorlach, M., and Anglister, J. (2003) Alternative Conformations of HIV-1 V3 Loops mimic beta hairpins in chemokines, suggesting a mechanism for coreceptor selectivity. *Structure 11*, 225–236.
18. Tugarinov, V., Zvi, A., Levy, R., and Anglister, J. (1999) A cis proline turn linking two beta-hairpin strands in the solution structure of an antibody-bound HIV-1_{IIIB} V3 peptide. *Nat. Struct. Biol. 6*, 331–315.
19. Tugarinov, V., Zvi, A., Levy, R., Hayek, Y., Matsushita, S., and Anglister, J. (2000) NMR structure of an anti-gp120 antibody complex with a V3 peptide reveals a surface important for coreceptor binding. *Struct. Fold Des. 8*, 385–395.
20. Rosen, O., Chill, J., Sharon, M., Kessler, N., Mester, B., Zolla-Pazner, S., and Anglister, J. (2005) Induced fit in HIV-neutralizing antibody complexes: evidence for alternative conformations of the gp120 V3 loop and the molecular basis for broad neutralization. *Biochemistry 44*, 7250–7258.
21. Rosen, O., Sharon, M., Quadt-Akabayov, S. R., and Anglister, J. (2006) Molecular switch for alternative conformations of the HIV-1 V3 region: implications for phenotype conversion. *Proc. Natl. Acad. Sci. U. S. A. 103*, 13950–13955.
22. Ghiara, J. B., Stura, E. A., Stanfield, R. L., Profy, A. T., and Wilson, I. A. (1994) Crystal structure of the principal neutralization site of HIV-1. *Science 264*, 82–85.
23. Rini, J. M., Stanfield, R. L., Stura, E. A., Salinas, P. A., Profy, A. T., and Wilson, I. A. (1993) Crystal structure of a human immunodeficiency virus type 1 neutralizing antibody, 50.1, in complex with its V3 loop peptide antigen. *Proc. Natl. Acad. Sci. U. S. A. 90*, 6325–6329.

24. Stanfield, R., Cabezas, E., Satterthwait, A., Stura, E., Profy, A., and Wilson, I. (1999) Dual conformations for the HIV-1 gp120 V3 loop in complexes with different neutralizing Fabs. *Structure 7*, 131–142.
25. Stanfield, R. L., Ghiara, J. B., Ollmann Saphire, E., Profy, A. T., and Wilson, I. A. (2003) Recurring conformation of the human immunodeficiency virus type 1 gp120 V3 loop. *Virology 315*, 159–173.
26. Stanfield, R. L., Gorny, M. K., Zolla-Pazner, S., and Wilson, I. A. (2006) Crystal structures of human immunodeficiency virus type 1 (HIV-1) neutralizing antibody 2219 in complex with three different V3 peptides reveal a new binding mode for HIV-1 cross-reactivity. *J. Virol. 80*, 6093–6105.
27. Bell, C. H., Pantophlet, R., Schiefner, A., Cavacini, L. A., Stanfield, R. L., Burton, D. R., and Wilson, I. A. (2008) Structure of antibody F425-B4e8 in complex with a V3 peptide reveals a new binding mode for HIV-1 neutralization. *J. Mol. Biol. 375*, 969–978.
28. Stanfield, R. L., Gorny, M. K., Williams, C., Zolla-Pazner, S., and Wilson, I. A. (2004) Structural rationale for the broad neutralization of HIV-1 by human monoclonal antibody 447−52D. *Structure (Camb) 12*, 193–204.
29. Huang, C. C., Tang, M., Zhang, M. Y., Majeed, S., Montabana, E., Stanfield, R. L., Dimitrov, D. S., Korber, B., Sodroski, J., Wilson, I. A., Wyatt, R., and Kwong, P. D. (2005) Structure of a V3-containing HIV-1 gp120 core. *Science 310*, 1025–1028.
30. Huang, C. C., Lam, S. N., Acharya, P., Tang, M., Xiang, S. H., Hussan, S. S., Stanfield, R. L., Robinson, J., Sodroski, J., Wilson, I. A., Wyatt, R., Bewley, C. A., and Kwong, P. D. (2007) Structures of the CCR5 N terminus and of a tyrosine-sulfated antibody with HIV-1 gp120 and CD4. *Science 317* 1930–1934.
31. Santiveri, C. M., Leon, E., Rico, M., and Jimenez, M. A. (2008) Context-dependence of the contribution of disulfide bonds to beta-hairpin stability. *Chemistry 14*, 488–499.
32. Hutchinson, E. G., Sessions, R. B., Thornton, J. M., and Woolfson, D. N. (1998) Determinants of strand register in antiparallel beta-sheets of proteins. *Protein Sci. 7*, 2287–2300.
33. Chakraborty, K., Durani, V., Miranda, E. R., Citron, M., Liang, X., Schleif, W., Joyce, J. G., and Varadarajan, R. (2006) Design of immunogens that present the crown of the HIV-1 V3 loop in a conformation competent to generate 447−52D-like antibodies. *Biochem. J. 399*, 483–491.
34. Conley, A. J., Conard, P., Bondy, S., Dolan, C. A., Hannah, J., Leanza, W. J., Marburg, S., Rivetna, M., Rusiecki, V. K., Sugg, E. E., et al. (1994) Immunogenicity of synthetic HIV-1 gp120 V3-loop peptide-conjugate immunogens. *Vaccine 12*, 445–451.
35. Cabezas, E., Wang, M., Parren, P. W., Stanfield, R. L., and Satterthwait, A. C. (2000) A structure-based approach to a synthetic vaccine for HIV-1. *Biochemistry 39*, 14377–14391.
36. FitzGerald, D. J., Fryling, C. M., McKee, M. L., Vennari, J. C., Wrin, T., Cromwell, M. E., Daugherty, A. L., and Mrsny, R. J. (1998) Characterization of V3 loop-Pseudomonas exotoxin chimeras. Candidate vaccines for human immunodeficiency virus-1. *J. Biol. Chem. 273*, 9951–9958.
37. Bryder, K., Sbai, H., Nielsen, H. V., Corbet, S., Nielsen, C., Whalen, R. G., and Fomsgaard, A. (1999) Improved immunogenicity of HIV-1 epitopes in HBsAg chimeric DNA vaccine plasmids by structural mutations of HBsAg. *DNA Cell Biol. 18*, 219–225.
38. Backstrom, M., Lebens, M., Schodel, F., and Holmgren, J. (1994) Insertion of a HIV-1-neutralizing epitope in a surface-exposed internal region of the cholera toxin B-subunit. *Gene 149*, 211–217.
39. Fontenot, J. D., Gatewood, J. M., Mariappan, S. V., Pau, C. P., Parekh, B. S., George, J. R., and Gupta, G. (1995) Human immunodeficiency virus (HIV) antigens: structure and serology of multivalent human mucin MUC1-HIV V3 chimeric proteins. *Proc. Natl. Acad. Sci. U. S. A. 92*, 315–319.
40. Scodeller, E. A., Tisminetzky, S. G., Porro, F., Schiappacassi, M., De Rossi, A., Chiecco-Bianchi, L., and Baralle, F. E. (1995) A new epitope presenting system displays a HIV-1 V3 loop sequence and induces neutralizing antibodies. *Vaccine 13*, 1233–1239.
41. Resnick, D. A., Smith, A. D., Gesiler, S. C., Zhang, A., Arnold, E., and Arnold, G. F. (1995) Chimeras from a human rhinovirus 14-human immunodeficiency virus type 1 (HIV-1) V3 loop seroprevalence library induce neutralizing responses against HIV-1. *J. Virol. 69*, 2406–2411.
42. Perham, R. N., Terry, T. D., Willis, A. E., Greenwood, J., di Marzo Veronese, F., and Appella, E. (1995) Engineering a peptide epitope display system on filamentous bacteriophage. *FEMS Microbiol. Rev. 17*, 25–31.
43. Oggioni, M. R., Medaglini, D., Romano, L., Peruzzi, F., Maggi, T., Lozzi, L., Bracci, L., Zazzi, M., Manca, F., Valensin, P. E., and Pozzi, G. (1999) Antigenicity and immunogenicity of the V3 domain of HIV type 1 glycoprotein 120 expressed on the surface of *Streptococcus gordonii*. *AIDS Res. Hum. Retroviruses 15*, 451–459.
44. Zolla-Pazner, S., Cohen, S. S., Krachmarov, C., Wang, S., Pinter, A., and Lu, S. (2008) Focusing the immune response on the V3 loop, a neutralizing epitope of the HIV-1 gp120 envelope. *Virology 372*, 233–246.
45. Vranken, W. F., Budesinsky, M., Fant, F., Boulez, K., and Borremans, F. A. (1995) The complete consensus V3 loop peptide of the envelope protein gp120 of HIV-1 shows pronounced helical character in solution. *FEBS Lett. 374*, 117–121.
46. Markert, R. L., Ruppach, H., Gehring, S., Dietrich, U., Mierke, D. F., Kock, M., Rubsamen-Waigmann, H., and Griesinger, C. (1996) Secondary structural elements as a basis for antibody recognition in the immunodominant region of human immunodeficiency viruses 1 and 2. *Eur. J. Biochem. 237*, 188–204.
47. Ofek, G., Tang, M., Sambor, A., Katinger, H., Mascola, J. R., Wyatt, R., and Kwong, P. D. (2004) Structure and mechanistic analysis of the anti-human immunodeficiency virus type 1 antibody 2F5 in complex with its gp41 epitope. *J. Virol. 78*, 10724–10737.
48. Cardoso, R. M., Zwick, M. B., Stanfield, R. L., Kunert, R., Binley, J. M., Katinger, H., Burton, D. R., and Wilson, I. A. (2005) Broadly neutralizing anti-HIV antibody 4E10 recognizes a helical conformation of a highly conserved fusion-associated motif in gp41. *Immunity 22*, 163–173.
49. Saphire, E. O., Parren, P. W., Pantophlet, R., Zwick, M. B., Morris, G. M., Rudd, P. M., Dwek, R. A., Stanfield, R. L., Burton, D. R., and Wilson, I. A. (2001) Crystal structure of a neutralizing human IGG against HIV-1: a template for vaccine design. *Science 293*, 1155–1159.
50. Calarese, D. A., Lee, H. K., Huang, C. Y., Best, M. D., Astronomo, R. D., Stanfield, R. L., Katinger, H., Burton, D. R., Wong, C. H., and Wilson, I. A. (2005) Dissection of the carbohydrate specificity of the broadly neutralizing anti-HIV-1 antibody 2G12. *Proc. Natl. Acad. Sci. U. S. A. 102*, 13372–13377.
51. Wu, X., Sambor, A., Nason, M. C., Yang, Z. Y., Wu, L., Zolla-Pazner, S., Nabel, G. J., and Mascola, J. R. (2008) Soluble CD4 broadens neutralization of V3-directed monoclonal antibodies and guinea pig vaccine sera against HIV-1 subtype B and C reference viruses. *Virology 380*, 285–295.
52. Van Herrewege, Y., Morellato, L., Descours, A., Aerts, L., Michiels, J., Heyndrickx, L., Martin, L., and Vanham, G. (2008) CD4 mimetic miniproteins: potent anti-HIV compounds with promising activity as microbicides. *J. Antimicrob. Chemother. 61*, 818–826.
53. Madani, N., Schon, A., Princiotto, A. M., Lalonde, J. M., Courter, J. R., Soeta, T., Ng, D., Wang, L., Brower, E. T., Xiang, S. H., Do Kwon, Y., Huang, C. C., Wyatt, R., Kwong, P. D., Freire, E., Smith, A. B., 3rd., and Sodroski, J. (2008) Small-molecule CD4 mimics interact with a highly conserved pocket on HIV-1 gp120. *Structure 16*, 1689–1701.
54. Kamber, B., Hartmann, A., Eisler, K., Riniker, B., Rink, H., Sieber, P., and Rittel, W. (1980) The synthesis of cystine peptides by iodine oxidation of *S*-trityl-cysteine and *S*-acetamidomethyl-cysteine peptides. *Helv. Chim. Acta 63*, 899–915.
55. Ratner, L., Haseltine, W., Patarca, R., Livak, K. J., Starcich, B., Josephs, S. F., Doran, E. R., Rafalski, J. A., Whitehorn, E. A., Baumeister, K., et al. (1985) Complete nucleotide sequence of the AIDS virus, HTLV-III. *Nature (London) 313*, 277–284.
56. Braunschweiler, L., and Ernst, R. R. (1983) Coherence transfer of Isotropic mixing: application to proton correlation spectroscopy. *J. Magn. Reson. 53*, 521–528.
57. Shaka, A. J., Keeler, J., and Freeman, R. (1983) Evaluation of a new broadband decoupling sequence: WALTZ-16. *J. Magn. Reson. 53*, 313–340.
58. Rucker, S. P., and Shaka, A. J. (1989) Broadband homonuclear cross polarization in 2D NMR using DIPSI-2. *Mol. Phys. 68*, 509–517.
59. Piantini, U., Sorensen, O., and Ernst, R. R. (1982) *J. Am. Chem. Soc. 104*, 6800–6801.
60. Sklenar, V., Piotto, M., Leppik, R., and Saudek, V. (1993) Gradient-tailored water suppression For H-1-N-15 Hsqc experiments optimized to retain full sensitivity. *J. Magn. Reson. Series A 102*, 241–245.

61. Piotto, M., Saudek, V., and Sklenar, V. (1992) Gradient-tailored excitation for single-quantum NMR spectroscopy of aqueous solutions. *J. Biomol. NMR 2*, 661–665.
62. Hwang, T. L., and Shaka, A. J. (1995) Water suppression that works. Excitation sculpting using arbitrary wave-forms and pulsed-field gradients. *J. Magn. Reson., Series A 112*, 275–279.
63. Delaglio, F., Grzesiek, S., Vuister, G. W., Zhu, G., Pfeifer, J., and Bax, A. (1995) NMRPipe: a multidimensional spectral processing system based on UNIX pipes. *J. Biomol. NMR 6*, 277–293.
64. Johnson, B. A. (2004) Using NMRView to visualize and analyze the NMR spectra of macromolecules. *Methods Mol. Biol. 278*, 313–352.
65. Neidig, K. P., Geyer, M., Gorler, A., Antz, C., Saffrich, R., Beneicke, W., and Kalbitzer, H. R. (1995) Aurelia, a program for computer-aided analysis of multidimensional NMR-spectra. *J. Biomol. NMR 6*, 255–270.
66. Herrmann, T., Guntert, P., and Wuthrich, K. (2002) Protein NMR structure determination with automated NOE-identification in the NOESY spectra using the new software ATNOS. *J. Biomol. NMR 24*, 171–189.
67. Roberts, G. C. K. (1993) *NMR of Macromolecules, a Parctical Approach*; Oxford University Press: New York.
68. Wishart, D. S., and Sykes, B. D. (1994) Chemical shifts as a tool for structure determination. *Methods Enzymol. 239*, 363–392.
69. Syud, F. A., Espinosa, J. F., and Gellman, S. H. (1999) NMR-based quantification of beta-sheet populations in aqueous solution through use of reference peptides for the folded and unfolded states. *J. Am. Chem. Soc. 121*, 11577–11578.
70. Stanger, H. E., and Gellman, S. H. (1998) Rules for antiparallel beta-sheet design: D-Pro-Gly is superior to L-Asn-Gly for beta-hairpin nucleation. *J. Am. Chem. Soc. 120*, 4236–4237.
71. Espinosa, J. F., Syud, F. A., and Gellman, S. H. (2002) Analysis of the factors that stabilize a designed two-stranded antiparallel beta-sheet. *Protein Sci. 11*, 1492–1505.
72. Syud, F. A., Stanger, H. E., Mortell, H. S., Espinosa, J. F., Fisk, J. D., Fry, C. G., and Gellman, S. H. (2003) Influence of strand number on antiparallel beta-sheet stability in designed three- and four-stranded beta-sheets. *J. Mol. Biol. 326*, 553–568.
73. Wuthrich, K. (1986) *NMR of Proteins and Nucleic Acids*; John Wiley: New York.
74. Cierpicki, T., and Otlewski, J. (2001) Amide proton temperature coefficients as hydrogen bond indicators in proteins. *J. Biomol. NMR 21*, 249–261.
75. Baxter, N. J., and Williamson, M. P. (1997) Temperature dependence of ^{1}H chemical shifts in proteins. *J. Biomol. NMR 9*, 359–369.
76. Vranken, W. F., Budesinsky, M., Martins, J. C., Fant, F., Boulez, K., Gras Masse, H., and Borremans, F. A. (1996) Conformational features of a synthetic cyclic peptide corresponding to the complete V3 loop of the RF HIV-1 strain in water and water/trifluoroethanol solutions. *Eur. J. Biochem. 236*, 100–108.

BI802308N